

Ecole Polytechnique

STEEM 2 Graduate Degree
Internship Final Report
Laboratoire de Météorologie Dynamique

Modeling the Impacts of Future Emission Scenarios on Air Pollution in Santiago, Chile

---

Student:
Rémy Lapere
remy.lapere@polytechnique.edu

Supervisors:
Sylvain Mailler
sylvain.mailler@lmd.polytechnique.fr
Laurent Menut
menut@lmd.polytechnique.fr



September 28, 2018

Abstract

The future of global climate as projected through IPCC RCP scenarios implies evolution in local weather patterns and changes in emission schemes of gaseous pollutants and particulate matter. In particular, the "baseline" RCP8.5 scenario provides estimates of pollutants emissions inventories in the coming years, which are driven by enforced environmental policies. Given the concern raised about air pollution in Chile in the recent years, we will focus on this part of the world, and more precisely around the metropolitan area of Santiago, where local extreme pollution events are usually encountered during winter time (fine particles hourly concentrations can reach up to 500 $\mu g/m^3$ in June/July). The fact that the basin of Santiago is surrounded by high mountains with a sharp topography is responsible for the accumulation of pollutants.
In this study we combine a meteorological model (Weather Research and Forecasting - WRF) and a chemistry-transport model (CHIMERE) in order to assess how pollutants and particulate matter (PM) atmospheric concentrations are likely to evolve at the 2050 horizon in Santiago metropolitan area. Our objective is to quantify the impact of projected changes in anthropogenic emissions on future air quality in Santiago, in order to provide guidance for local emissions control policies.
First, we recreate recently observed air quality in Chile (austral winter 2016) with WRF-CHIMERE, in order to validate our model configuration. Then we project pollutants concentrations under IPCC RCP8.5 and RCP2.6 scenarios for the same season at the 2050 horizon, and compare them with 2000 levels. Ultimately, our findings include reductions of $PM_{2.5}$ and NO_x concentrations in both scenarios over Santiago. RCP2.6 scenario shows much better improvements in air quality although its main focus is put on GHG emissions mitigation.

Keywords
Atmospheric Pollution • WRF • CHIMERE • Regional Climate • Chile • IPCC RCP Scenarios

Contents

Abstract **1**

1 Introduction **3**
1.1 Santiago de Chile . . . 3
1.2 Past and Future Trends in Chile . . . 5
1.2.1 Air Quality . . . 5
1.2.2 Meteorology and Climate . . . 5
1.2.3 Demography and Economy . . . 6
1.2.4 Emissions . . . 7
1.3 Atmospheric Chemistry Basics . . . 9
1.4 Chemistry-Transport Models . . . 10
1.5 Challenges in Modeling Santiago Area . . . 11
1.6 Assessing the Impacts of RCP Scenarios on Air Quality . . . 11

2 Methodology **15**
2.1 Geographic Domain and Time Period Definition . . . 15
2.2 Models Used for the Study . . . 16
2.2.1 Meteorological Model - WRF . . . 16
2.2.2 Chemistry-Transport Model - CHIMERE . . . 16
2.2.3 Anthropogenic Emissions Model - EDGAR-HTAP . . . 17
2.2.4 RCP Emission Scenarios . . . 18
2.3 Model Input Data and Observation Measurements . . . 19
2.3.1 Land Data . . . 19
2.3.2 *In-situ* Data . . . 19

3 Results **21**
3.1 Simulated Meteorology - 2016 . . . 21
3.2 Simulated Concentrations - 2016 . . . 26
3.3 Simulated Concentrations - 2050 . . . 31

4 Conclusion **35**

1. Introduction

Air quality has become a major concern, especially in urban areas, as it constitutes a critical health driver among living species (human beings, animals and plants). Despite the difficulty to quantify exactly these effects (Cohen et al., 2017), a recent report by the World Health Organization estimates that "around 7 million people die every year from exposure to fine particles in polluted air" (World Health Organization, 2018). This would make air pollution one of the deadliest factors to human beings. In consequence, local governments need accurate guidance to take action aiming to improve urban air quality. In addition, the impacts on health of air pollution correlate to a substantial economic cost. In France, it is estimated that its total burden over the health-care system is in the range of EUR 1 to 2 billion per year (Rafenberg et al., 2015). Worldwide, this cost could even represent up to 1% of global GDP, i.e. around USD 2.6 trillion annually (OECD, 2016). Concerns surrounding air quality are particularly strong in Latin America, where "a more cohesive and sustained community of atmospheric scientists is needed [...] to address the pressing issues of air quality and climate change" (Andrade-Flores et al., 2016). The PAPILA European project gathering researchers from Latin America and Europe (European Commission, 2018) aims to serve this purpose, and constitutes a framework to which this study aims to contribute.

Climate change and air quality are closely intertwined issues. First, changes in climate characteristics (temperature, precipitations, winds) can affect the formation, transport and destruction of gaseous and particulate pollutants, whether issued from anthropogenic (traffic, cook-stoves, industry...) or natural sources (dust, fire, lightning...). Second, air pollutants (PM and Ozone (O_3) for instance) have an impact on earth radiative balance through direct (solar radiation scattering, greenhouse effect) and indirect (change in clouds properties) effects, which leads to a significant contribution to climate change. Finally, Greenhouse Gases (GHG) and air pollutants usually share common anthropogenic sources and are mainly co-generated. For instance, burning fuel in a car both emits Carbon Dioxide (CO_2) and Nitrous Oxides (NO_x) at the same time (Zhang et al., 2016). Thus, as climate policies seek to control GHG emissions, they will by the same token affect future air quality as well.

As a result of the two points aforementioned, it is key to be able to anticipate the effects of climate change mitigation policies (which are currently under the spotlights in each Conference Of the Parties) on future air quality conditions. In this respect, the present study assesses changes in atmospheric pollution levels in 2050 implied by IPCC RCP8.5 and RCP2.6 scenarios hypotheses, with a specific focus on the metropolitan region of Santiago de Chile. Section 1 introduces the particular characteristics of the region of Santiago and details the goal of the study. Section 2 describes the methodology used in order to build the simulation and extrapolate IPCC emissions scenarios. Section 3 presents the results obtained with the model, reproducing 2016 austral winter as a starting point, and running the 2050 horizon simulation, and discusses these results. Section 4 concludes on this study.

1.1 Santiago de Chile

Chile is a South American Andean country, comprising the Atacama desert in the North (implying mineral dust emissions - Ginoux et al., 2012), Pacific ocean in the West (leading to sea-salt emissions and transport towards the continent - Makowski Giannoni et al., 2016), and the Andes cordillera in the East (preventing part of west-east air transport). In particular, Chile's capital city, Santiago (33.5°S, 70.5°W, 500m a.s.l.) is surrounded by the Andes in the East with mountain peaks up to more than 5000m, less than 40km away from downtown, and the Chilean Coastal Range in the West which shows summits up to 1500m, even closer to the city area (Figure 1). This region is therefore of great interest: this geographic situation leads to atmospheric pollutants accumulation, since most of the emissions of the area will remain trapped above the city between these two mountain ranges and will not be able to transport farther, as can be seen on Figure 1. Combined with energy consumption habits in the region (cook-stoves, residential heating with wood burning, car driving...) leading to high levels of pollutants and aerosols emissions, this yields pollution levels among the highest in the world. That is why very stringent policies against pollutants emissions are required, and currently designed by the Chilean government in order to prevent catastrophic health impacts on the 7 million people living in the area (Ministerio del Medio Ambiente, 2018). Moreover, since the Andes mountains are close to the city, aerosols and pollutants emitted in the vicinity of Santiago reach the glaciers of the cordillera, with a significant impact of Black Carbon (BC) on the Andean cryosphere, changing ice albedo and composition thus leading to accelerated melting which

may contribute to ecosystems destruction and climate change (Molina et al., 2015). "Cookstoves in these urban regions [...] could have a significant impact on the rapid melting of snow and ice shown by the Andean tropical glaciers. Traffic emissions from diesel vehicles may also prove a significant source of black carbon" (International Cryosphere Climate Initiative, 2018). Transport of pollution downwind from Santiago also have potential impacts on cloud properties over the Pacific Ocean (Saide et al., 2012).

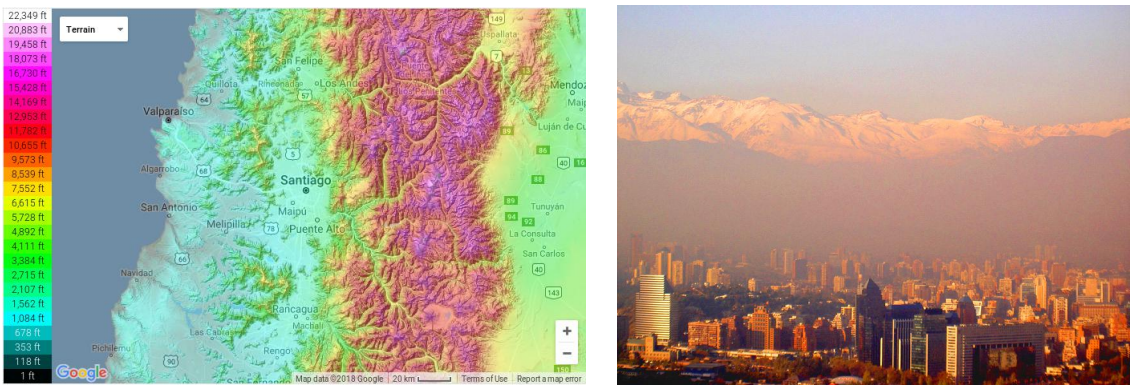


Figure 1: Left: Map of the region of Santiago de Chile - source *http://en-in.topographic-map.com* // Right: pollution event in Santiago *© Ueslei Marcelino/Reuters.*

Following Michael Greenstone's work at the Energy Policy Institute at the University of Chicago, pollution impacts on health can be summarized by the so-called Air Quality Life Index (AQLI) (Energy Policy Institute at the University of Chicago, 2017). The AQLI is a derivative of an index commonly used by epidemiologists and air quality researchers called Disability-Adjusted Life Year (DALY - see World Health Organization). The AQLI index compares air quality measurements to World Health Organization (WHO) recommended standards, and estimates, for each region of the world, how many years of life per capita could be saved if these standards were to be met. As shown in the map below, though still far from Chinese and Indian extremely concerning situations, Chile's index is comparable to some Asian and African countries, with an annual mean 22.2 $\mu g/m^3$ $PM_{2.5}$ concentration, corresponding to a potential saving of 1.37 life years per capita. NB: $PM_{2.5}$ are particulate matter aerosols with a radius smaller than 2.5 μm.

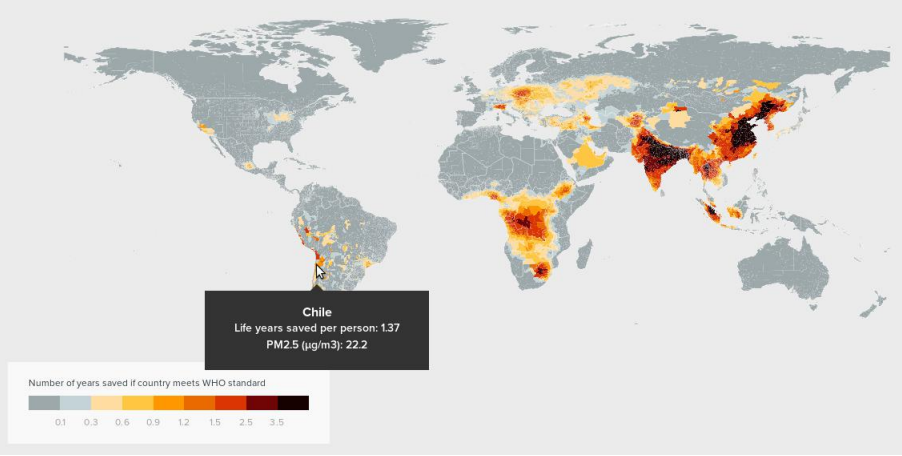


Figure 2: Air Quality Life Index World Map - source Energy Policy Institute at the University of Chicago.

According to the study by Greenstone (which detailed methodology can be found in Chen et al., 2013), that would make Chile the tenth deadliest country in the world in terms of $PM_{2.5}$ air pollution. Only India, China, Pakistan, Tajikistan, Thailand, Laos, Congo, Democratic Republic of Congo and South Africa show a higher life years saving potential. Among these top ten countries, Chile has by far the highest Human Development Index (United Nations Development Programme, 2016), making it likely more suitable for quick win political actions towards pollution mitigation.

1.2 Past and Future Trends in Chile

1.2.1 Air Quality

For some years now Santiago's policy makers have been concerned by air quality in the metropolitan area. Some measures have thus been enforced to reduce atmospheric pollutants emissions, in particular the "Atmospheric Decontamination Plans" (Ministerio del Medio Ambiente, 2018). We can see on Figure 3 below, showing yearly mean concentrations for 4 pollutants measured in downtown Santiago, that these policies have started having an impact in the last two decades, with a significant decrease. However, mean levels seem to stabilize in the recent years and remain quite high compared to WHO guide values, which leaves room for improvement in the future [NB: according to Osses et al., 2013 the station "Parque O'Higgins" we show here, located downtown - see map in Section 2 - is the most representative of the average air quality situation in Santiago]. This improvement can be achieved thanks to enhanced modeling for more enlightened policy decisions through the science-policy interface (Gallardo et al., 2018). In terms of health impact, new targets for $PM_{2.5}$ concentrations were established in 2012 that are expected to save up to $41 billion in health care expenses over the period 2012-2031 (Ministerio del Medio Ambiente, 2012).

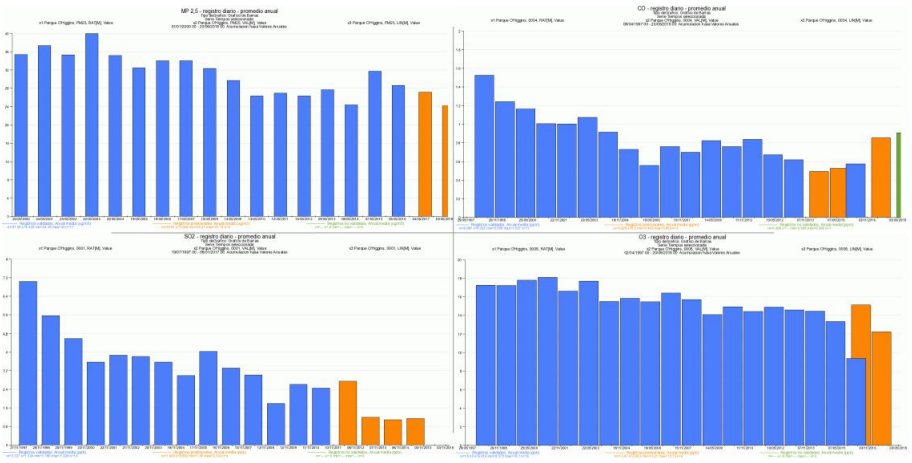


Figure 3: Top Left: $PM_{2.5}$ yearly average concentrations since 2000 // Top right: CO yearly average concentrations since 1997 // Bottom Left: SO_2 yearly average concentrations since 1997 // Bottom right: O_3 yearly average concentrations since 1997 - source Ministerio del Medio Ambiente, Parque O'Higgins station.

1.2.2 Meteorology and Climate

Given its elongated shape, Chile encompasses a very wide variety of climates along the country, from arid deserts in the North to glacial lands in the South. Santiago area, located in central Chile is characterized by a Mediterranean climate, with average monthly temperatures around 19.5°C in summer and 7.5°C in winter, and with very few precipitations in summer and a relatively high 70 to 100mm a month in winter time (World Meteorological Organization, 2017 and Figure 4). Compared to a European capital city like Paris (which is very well known in terms of Chemistry-Transport modeling), Santiago shows a smaller seasonal variability in temperatures - Paris maximum and minimum monthly average temperatures are 20°C and 4°C, respectively. On the contrary, precipitations in Santiago have a very strong seasonality, which is not the case in Paris where precipitations are more or less constant all year long. From a historical point of view in terms of temperature anomalies, Paris shows a higher year-to-year variability, but on the whole, the trend of a roughly 1°C warming since 1900 is common to both cities. This number is huge but probably attributable to the sharp increase in urbanization leading to an enhanced urban heat island effect.

As for Chile as a whole, according to Falvey and Garreaud, 2009, surface temperature trends over the last 25 years of the 20^{th} century in South America show a decrease of up to -0.25°C/decade westward of the Andes along the Pacific coast, while a symmetric warming is found along the Atlantic coast. They show for instance that there is a temperature deviation gradient in the east-west direction in Chile: the closer the location is to the Pacific ocean, the smaller the warming. They even find a decreasing temperature trend on Juan Fernandez, a Chilean island in the Pacific ocean. This study estimates a +0.28°C/decade in the Western Andes, +0.18°C/decade in Central Chile, and -0.18°C/decade in Juan Fernandez.

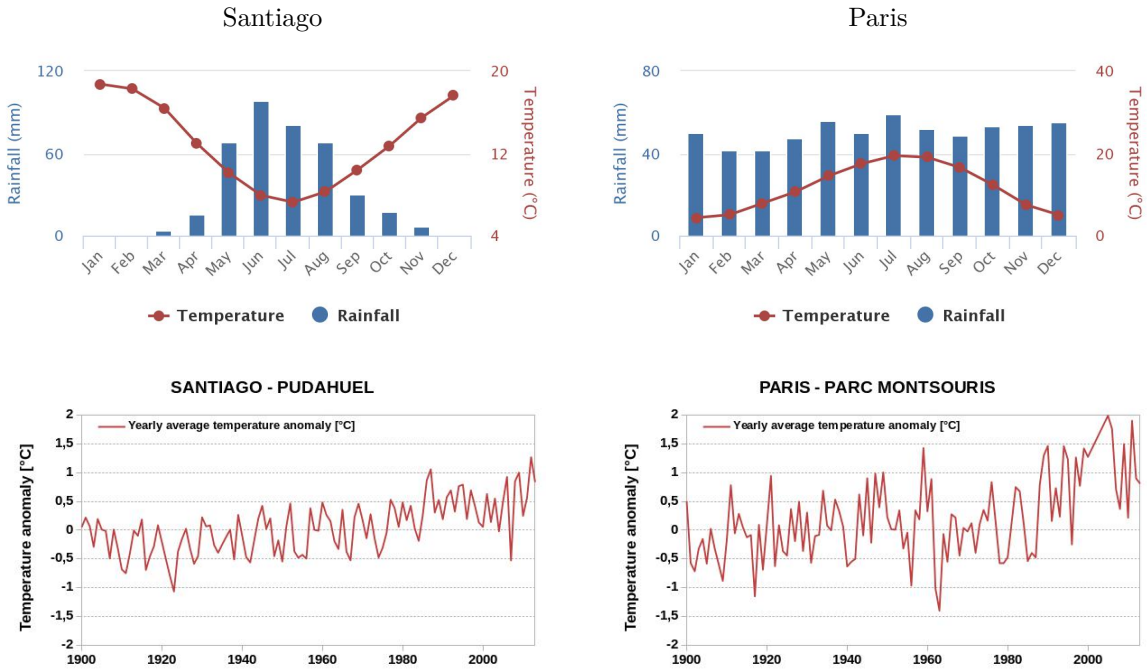


Figure 4: Top: monthly average historical temperatures and precipitations for Santiago and Paris (1901-2015) - source The World Bank Group // Bottom: yearly temperature anomalies in downtown Santiago and Paris over the last century - source Berkeley Earth.

- Wind systems:
  - Central Chile is situated at the convergence zone between large scale atmospheric circulation Hadley and Ferrel cells, around 30° South. This junction forms the subtropical high-pressure belt, where high pressure air descends to the ground (Encyclopædia Britannica), which leads to the prevalence of dry conditions: a general subsident air motion prevents air from rising thus not allowing humid air from the ground to go in altitude and get colder, expand, condensate and eventually form raindrops. Rains are then inhibited. Another consequence of this high-pressure zone is low-intensity winds, which do not allow significant evacuation of pollution out of Santiago.
  - Diurnal wind cycle (Airparif, 2006): at night, wind blows mainly in the East-West direction, so that in the morning, polluted air masses concentrate in the Western area of Santiago. Contrarily, in the afternoon, winds change directions and pollutants are transported toward the East, to the foothills of the Andes. Winds coming from outside Santiago basin blow mainly South and South-West, transporting pollution emitted by industries toward downtown Santiago.
  - Seasonal wind cycle (Airparif, 2006): during summer, the diurnal wind speeds amplitude is higher, enhancing evacuation of pollutants. In winter on the contrary, the basin of Santiago is poorly ventilated which leads to pollution peaks.
- Given its wide Pacific Ocean coast, Chile's climate is influenced by the Pacific Ocean cell (air motions above the Pacific ocean along the East-West axis - Collier, 2016), and thus El Niño Southern Oscillation (ENSO): El Niño years correlate with rainfalls above average in central Chile during winter (which can improve aerosol scavenging), and with dry conditions in summer. La Niña years do exactly the opposite. Thus, regional and large-scale circulation during severe rainfall conditions in Chile are closely related to the extreme ENSO phases (Montecinos and Aceituno, 2003).

1.2.3 Demography and Economy

Based on Figure 5 below, which is composed of elements from several studies, we have an overview of past and expected population evolution and economic growth of Chile:

- The growth of population in Chile is currently slowing down, with an expected decrease starting around 2050, when a maximum of 21 million inhabitants is reached. In other words, the 2050 horizon in which this study is interested is likely to be a climax in terms of risks of population exposure to air pollution.
- Santiago Metropolitan area concentrates almost 40% of Chile's total population, and an additional 10% of the population lives in the 2^{nd} and 3^{rd} biggest cities (which are near Santiago). The very high rate of urbanization of Chile makes the previous point even more critical, and the sprawl is expected to go on.
- The slowing growth of GDP observed in the recent years is expected to start increasing steadily back again in the coming years. The economy of Chile is thus expected to develop, and since development and pollution issues are often intertwined, close attention must be paid to environmental policies in the next few years.

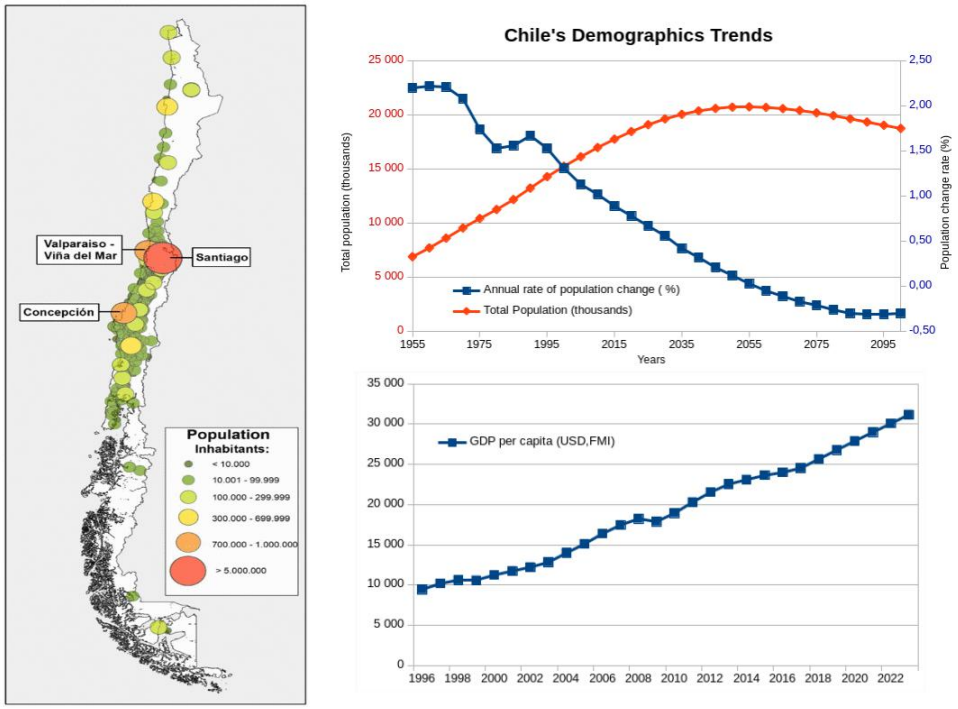


Figure 5: Left: Spatial Distribution of Population in Cities of Continental Chile with more than 5000 inhabitants in 2012 - source Gallardo et al., 2018 // Top right: Evolution and Future of Chile's population- source United Nations // Bottom right: Evolution of Chile's GDP per capita - source Banco Central de Chile.

1.2.4 Emissions

According to Barraza et al., 2017 a significant decrease in absolute median levels of $PM_{2.5}$ concentrations in the last two decades have been observed in Santiago (Figure 6). The drastic cut of emissions from copper smelters and coastal sources seems to be the main factor explaining this fall. Primary technological mitigation policies addressing vehicle emissions have also helped decrease transportation emissions (Gallardo et al., 2018), but the share of this sector in total $PM_{2.5}$ emissions in Santiago raised from 24% in 1998-1999 to 39% in 2011-2012, meaning that it still remains a major leverage point for mitigation policies.

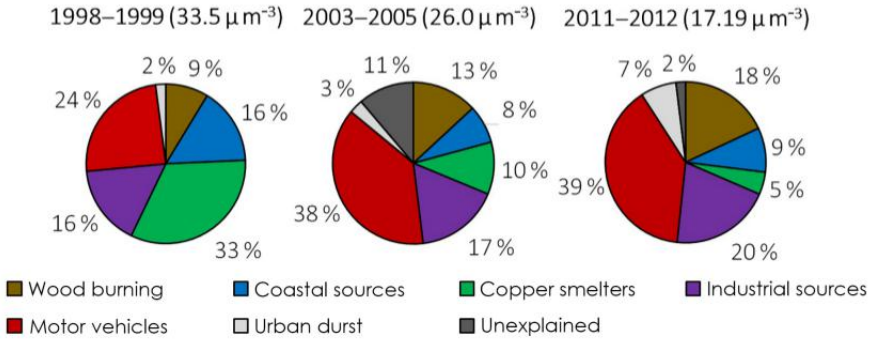


Figure 6: Relative contribution of sources to $PM_{2.5}$ levels in late 20th / early 21st century - source Barraza et al., 2017.

Based on the data provided by emission inventories from EDGAR-HTAP (see Section 2.2.3), we can clearly identify Santiago as the main emitting area of the region for most types of primary atmospheric pollutants (with Valparaíso and Rancagua significant emission zones as well). Figure 7 below shows 2010 emissions maps for nitrogen oxide, carbon monoxide, black carbon and sulfur dioxide in Santiago area. We can see on the scales of these graphs the magnitudes of emission rates (molecule/cm^2/s) of the four species, where CO - currently used as a proxy in Santiago to forecast $PM_{2.5}$ events (Saide et al., 2016) - is the most emitted species with up to 10^{15} molecules/cm^2/s, and fine BC is three orders of magnitude less at 10^{12} molecules/cm^2/s. As a comparison for these numbers, Petetin et al., 2015 find emission rates of NO_x and BC in 2009 for Paris area up to 10^{13} molecules/cm^2/s and 10^{11} molecules/cm^2/s, respectively, i.e. roughly one order of magnitude less than what we have for Santiago.

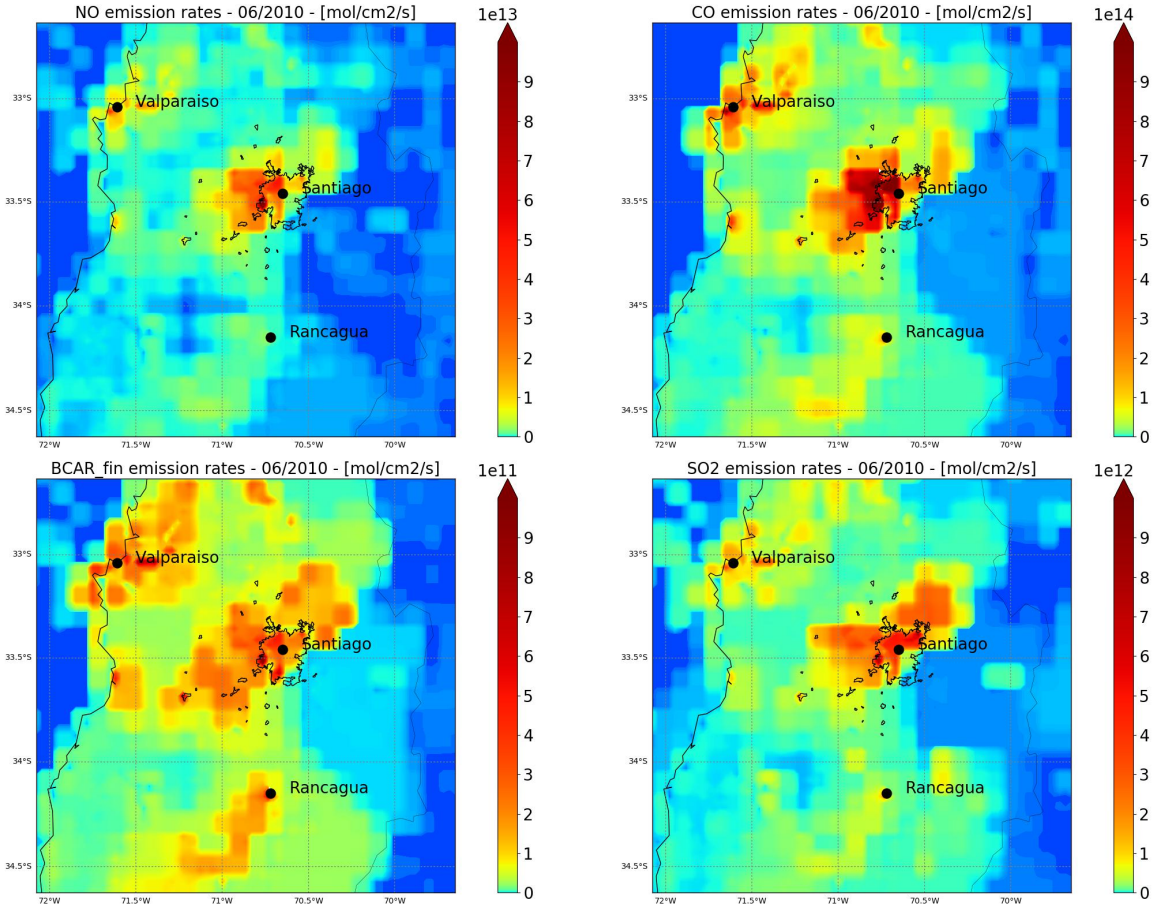


Figure 7: Emission Maps from 2010 HTAP Inventory for Santiago Area - data from Task Force on Hemispheric Transport of Air Pollution.

1.3 Atmospheric Chemistry Basics

Below are introduced a few notions of atmospheric chemistry that are important for our study and that can be useful for the uninitiated reader.

- The Planetary Boundary Layer (PBL) is the lowest part of the atmosphere, under the direct influence of the Earth surface, and governed by turbulent motion and fast vertical mixing. As it constitutes the air layer in which human beings live, it is the main target of modeling for atmospheric chemists with a view to policy recommendations. The PBL height determines the thickness of the polluted layer and its diurnal cycle governs the injection of pollutants into the free troposphere (Figure 8).
- Atmospheric inversions (or thermal inversions) occur when the lowest air layers are cooler than the layers higher up (Figure 9). These conditions create extremely stable and shallow boundary layers that are favorable to peak pollution events. This phenomenon happens mostly in cold winter time, and can be caused by four main events in Santiago: the Pacific anticyclone presence, coastal depressions, hot air motions in altitude or thermal radiative inversions (Airparif, 2006).
- There are many sources of air pollutants, but their sinks are quite well identified:
  - For Particulate Matter, deposition (wet or dry) is the main removing process from the air. In particular, cloud and rain scavenging are efficient processes to do so. Eventually, even without rain and in a dry air, aerosols (especially coarse ones) will fall to the ground. This is called dry deposition.
  - For gaseous species it is more complex, but for many of them the two main sinks in the atmosphere are the oxidation by radicals, in particular by hydroxyl (OH), and dry deposition in plants (e.g. O_3).
- Transport of pollutants can occur through several types of air mass motions. Large-scale circulations may transport mineral dust particles from deserts to areas far away, as is the case with Saharan dust that feeds plants in Amazon (Yu et al., 2015). Smaller scale wind advection also occurs, which is observed in France in Paris area for instance, where summer O_3 pollution peaks are located outside of the main emitting area, downstream dominant wind motions (Airparif, 2001). Vertical mixing and turbulence in the PBL also contribute to the transport of pollutants.
- Primary and Secondary pollutants: primary pollutants are species that are emitted into the atmosphere directly in their final form (e.g. NO_x , CO, soot, dust...). Secondary pollutants are created via the combination of the emission of their precursors and meteorological conditions (secondary aerosols, ozone...). Over Europe for instance, secondary PM share in $PM_{2.5}$ concentrations are estimated to be way more important than primary (European Environment Agency, 2009). Secondary PM are also significant in Santiago: according to Villalobos et al., 2015, in winter at least 40% of $PM_{2.5}$ concentrations are made of secondary PM, and this share can go as high as almost 60% in fall and spring. Hence the need for chemistry-transport modeling, since emissions modeling only captures primary pollutants.

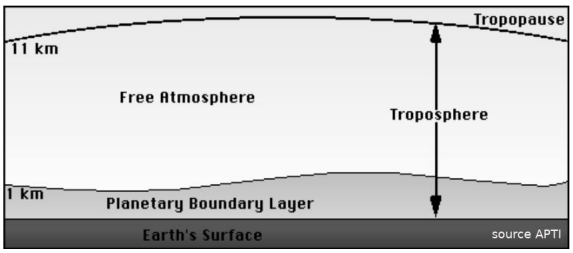


Figure 8: Planetary Boundary Layer schematic.

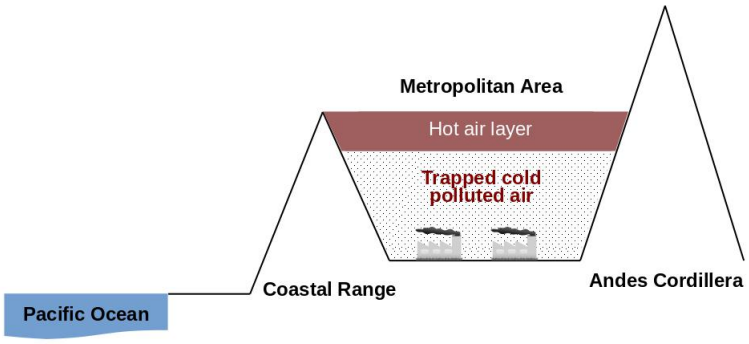


Figure 9: Thermal Inversion over Santiago schematic.

1.4 Chemistry-Transport Models

A Chemistry-Transport Model (CTM) is composed of several modules that articulate to simulate atmospheric composition at a regional scale based on meteorology and emissions. Three main components are used, namely meteorological fields (that can be coupled -online- or not -offline- to chemistry), emissions inventory models (either static or dynamical), and chemistry-transport computations. Figure 10 below shows a simplified scheme of this operational sequence, that we will detail more in section 2.

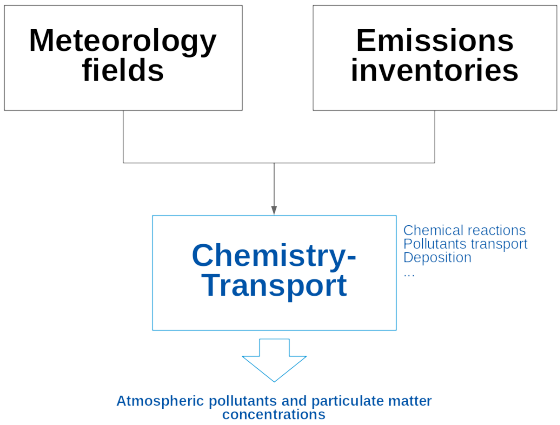


Figure 10: Chemistry Transport Model scheme.

The idea of the chemistry-transport part (blue box above) is to simulate concentrations of pollutants and particles based on the discretization along space and time (finite elements) of the following equation that describes the evolution of air concentrations for a species i:

$$\frac{\partial c_i}{\partial t} = -\underbrace{\nabla \cdot (\mathbf{V} c_i)}_{\substack{\text{Wind} \\ \text{advection}}} + \underbrace{\nabla \cdot (\mathbf{K} \nabla c_i)}_{\substack{\text{Turbulent} \\ \text{diffusion}}} + \underbrace{\chi(c_i, c_j, .., T..)}_{\substack{\text{Chemical and} \\ \text{physical processes}}} - \underbrace{P_i}_{\text{Sinks}} + \underbrace{S_i}_{\text{Sources}} \quad (1)$$

where:

- c_i is the concentration of species i,
- $\mathbf{V}$ is the horizontal wind speed vector, interpolated from the modeled meteorology fields,
- $\mathbf{K}$ is the vertical wind speed vector, interpolated from the modeled meteorology fields,
- χ gathers all the chemical processes (formation, transformation...) linked to species i and interacting species,
- T is the temperature, interpolated from the modeled meteorology fields,

- P_i and S_i are sinks and sources processes, respectively. S_i is interpolated from the modeled emissions, P_i is modeled in the chemistry-transport module

NB: we can see from this equation that such a model is very sensitive to meteorology as well as emissions inventories modeled data.

In this study we use CHIMERE that is developed at LMD, but other well-known CTMs include WRF-Chem by NOAA, GEOS-Chem by Harvard University and Dalhousie University, CMAQ by the US Environmental Protection Agency (EPA), EURAD-IM by the university of Cologne (FRIUUK), CAMx developed by Ramboll Environ in the U.S., LOTOS-EUROS by TNO in Europe...

1.5 Challenges in Modeling Santiago Area

As mentioned previously, the region of Santiago features a very complex topography, leading to modeling challenges. Indeed, a CTM relies on a grid-based representation, which resolution corresponds to the smallest distinguishable unit. Over areas of several hundreds of kilometers, stability and computation time constrain the maximum resolution, which in our case is around 2km by 2km. As a result, over a sharp mountainous terrain, properties of the ground might change a lot over 2 kilometers, so that our grid resolution might be insufficient to adequately capture valleys and peaks, thus mismodeling air motions and temperatures for instance, by lack of spatial accuracy.

Another limitation we have to face is the fact that emissions are static with an inventory as of 2010 (see Section 2), and at a spatial and temporal resolution that is coarser than our grid / time steps. Downscaling and interpolation are therefore performed on these emissions inventories, but still are a source of error that makes our simulation less likely to produce accurate results, in particular for pollution peaks attributed to exceptional emission levels.

In addition, the method commonly used to validate the model outcomes is to compare to on-site observations. However, the measurement network in the area of Santiago is not fully developed yet, in particular in terms of availability of vertical profiles of meteorological variables and pollution. As a result, we are able to compare the model to measurements only over a limited number of places, and for limited time windows and altitudes.

As a consequence, a significant part of the work focuses on finding the appropriate grid resolution, nudging frequency and physics schemes in order to be able to reproduce a recent past period, meeting numerical stability and run time criteria. In particular, simulation results are very sensitive to meteorology, so that setting the most appropriate configuration for this part, which offers a lot of possibilities, is of great importance. When obtaining a "satisfactory" configuration, we will need to evaluate the uncertainties linked to the model biases induced by the complex terrain, which will allow us to quantify the uncertainty associated with our projection results.

1.6 Assessing the Impacts of RCP Scenarios on Air Quality

The general idea of this study is to assess potential upcoming air pollution levels in Santiago at the 2050 horizon. To do so, we consider that likely futures lie between the two extreme IPCC RCP scenarios: RCP2.6 and RCP8.5. Then we run simulations based on emission levels anticipated by these scenarios. The detailed methodology is described in the next section. Several studies have already been conducted on similar questions over Europe, the U.S. and Asia (e.g. Colette et al., 2013, Zhang et al., 2017 and Li et al., 2016, respectively). However, to our knowledge no literature exists on this particular topic for Santiago, nor the Latin American region generally speaking. Though some CTM simulations have already been made on some South American countries (Mazzeo et al., 2018 or García Ferreyra et al., 2016 for instance), such a projection along IPCC scenarios has not been performed yet over this region of the world. Conducting such studies regarding the impacts of policies on future air quality conditions is one of the main needs for chemistry transport models (and more generally climate models). As they provide an assessment of policies that could be implemented, they represent a powerful tool for guidance in policy making and a crucial field of the science-policy interface (Gallardo et al., 2018).

RCP2.6 and RCP8.5 scenarios assumptions and methodologies are described in van Vuuren et al., 2011 and Riahi et al., 2011, respectively. Below are summarized a few interesting features of these scenarios relating to air quality.

RCP2.6 scenario: this scenario is representative of the mitigation scenarios aiming to limit the increase of global mean temperature below 2°C, implying radiative forcing levels of greenhouse gases around 2.6W/m^2 at the 2100 horizon. This is the most stringent RCP scenario. This path needs rapidly decreasing energy demand, stabilizing world population, and cleaner energy sources in order to reach a negative GHG emission balance before 2100. RCP2.6 does not really focus on air quality policies, since effort is mainly put on GHG emissions. The air pollution scenario provided is mainly a co-product of the GHG scenario, without much dedicated actions considered.

RCP8.5 scenario: this is the so-called "baseline" scenario, where no specific climate mitigation target is implemented, energy demand keeps on growing along with world population, and clean energy sources are not developing. Thus, it leads to high GHG emissions and high radiative forcing (8.5W/m^2) at the 2100 horizon. Co-benefits on air quality from GHG mitigation policies seen in RCP2.6 are thus not present here. However, the methodology for this scenario embeds a dedicated path regarding air quality policies implementation. In particular, places of the world with high pollution exposures (i.e. highly populated and polluted at the same time) are considered to take major actions in order to mitigate air pollution issues in the coming decades.

Figure 11 shows these scenarios for BC and NO_x emissions for the world, split by emission sectors.

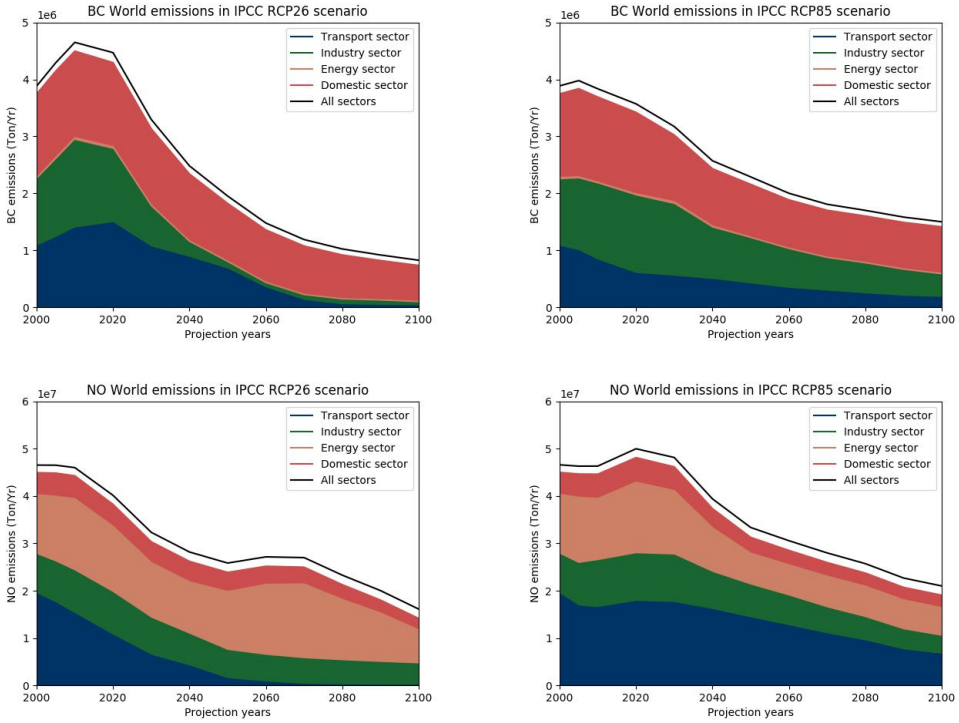


Figure 11: BC (top) and NO (bottom) World emissions scenarios by sector under RCP2.6 (left) and RCP8.5 (right) - data from IPCC.

Figure 12 shows the same graphs limited to the grid cell corresponding to Santiago area. We can see on this figures that:

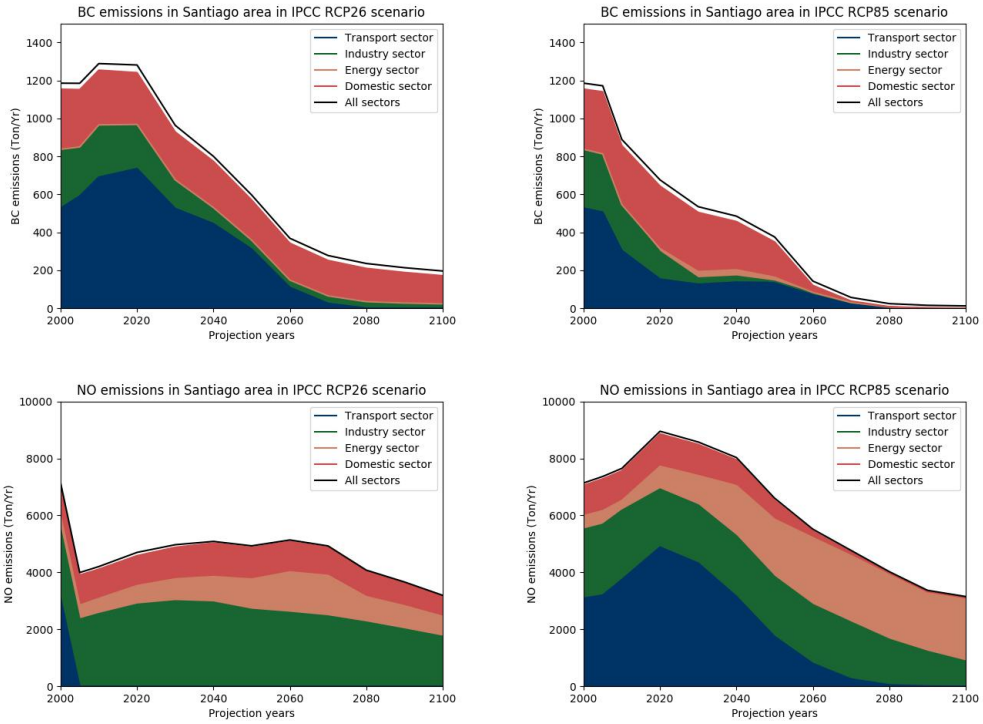


Figure 12: BC (top) and NO (bottom) emissions scenarios in Santiago area ([33.75°S, 71.25°W] to [33.25°S, 70.25°W]) by sector under RCP2.6 (left) and RCP8.5 (right) - data from IPCC.

- As of 2000, the main contributor for Black Carbon (BC) emissions is the transport sector, although in the future, in both scenarios, its share is likely to plummet and become comparable to the domestic contribution at the 2050 horizon. It is worth noting on this graph, that the expected level of BC emissions as of 2050 is smaller under the less climate-friendly scenario (RCP8.5). In other words, the RCP2.6 scenario that seeks to cut drastically GHG emissions leads to higher BC emissions than the business-as-usual scenario. The contrast is even bigger at the 2100 horizon where BC emissions are annihilated in RCP8.5 but remain substantial, in particular in the domestic sector, in RCP2.6.

- For Nitrogen Oxide (NO), RCP2.6 scenario does not contain projection data for the transport sector's emissions over the region we are interested in, unfortunately. We can see that all the other sectors remain more or less constant throughout the scenario. At the global scale, RCP2.6 shows a contribution of the transport sector to NO emissions that is very close to 0 as of 2050 (Figure 11 - bottom left). In this respect, we make the assumption that it goes the same way for Santiago, and assume that NO emissions by transport are indeed null as of 2050. This approximation is a little rough but still seems consistent with the global scenario. In RCP8.5 scenario, we can see that the energy sector is emitting more at the 2050 horizon, while transport and domestic sectors decrease and industry remains steady. Given its sharp drop in the transport sector emissions of NO, RCP2.6 scenario is likely to be a lower NO emitter than RCP8.5.

The BC graphs might be quite surprising at first glance since GHGs and pollutants such as BC are usually correlated. We would expect RCP2.6 scenario to show greater decrease in BC than RCP8.5, as it is the case for GHGs. However, this phenomenon can be explained by methodological differences between the two scenarios. As mentioned earlier, RCP2.6 does not integrate any air pollution targeting policies and focuses only on co-benefits from GHGs emission mitigation policies. What's more, the pollutants emissions computed at the country level are linearly downscaled based on land-use only, regardless of the dynamics of each area regarding air pollution. Contrarily, RCP8.5 includes air pollution mitigation scenarios and bases its downscaling on pollution exposures, i.e. the most polluted highly populated places will take critical action in order to tackle air quality issues. As a result, for the case of Santiago which is a highly populated and polluted area, RCP8.5 integrates a sharp decrease in BC emissions based on the high

probability that strong policies will be implemented in such a place. Despite being more energy demanding and more GHG emitting, RCP8.5 for Santiago is likely better for air quality than RCP2.6 where efforts are mainly focused on GHGs. This strengthens the idea that local specific features of Santiago drive the particularly counter-intuitive observations made in the previous figure. For instance, this may have to do with wood burning habits for energy production in the region, that are neutral in terms of GHG emissions (on the condition that wood resources are sustainably managed) and thus desirable for climate change mitigation in scenario RCP2.6, but emit a lot of BC, not always filtered. This shows potential negative impacts of climate change mitigation policies on air quality. Consequences on air quality will highly depend on spatial and temporal emission patterns though.

2. Methodology

2.1 Geographic Domain and Time Period Definition

The region of interest for this study is Santiago and its surroundings. In order to have a good representation of both regional and local transport and chemistry, we design two domains (Figure 13). The large one (white boundaries on the left-hand map) encompasses the whole region, from Atacama desert in the North down to Patagonia in the South. From West to East it comprises the Pacific Ocean Coasts right to the Southern Andes. This domain is designed to be able to account for potential long range aerosols transport from remote places (ocean, desert, forests...) up to the metropolitan area. Two grid resolutions are tested for this domain: 15km and 10km. The small high-resolution domain (red square on the left-hand map) focuses on Santiago metropolitan area but also encompasses other major cities such as Valparaíso and Rancagua. This domain is a square of 225 x 225km, gridded with a 3km resolution when the large domain is at the 15km resolution, and a 2km resolution otherwise (see right-hand map in Figure 13).

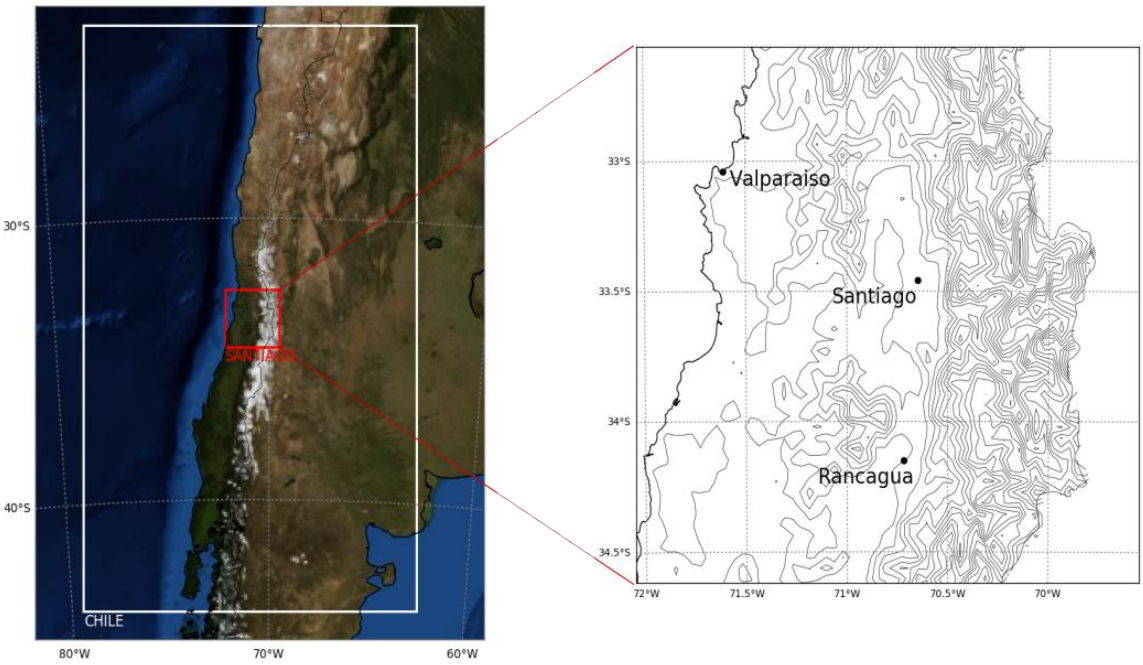


Figure 13: Domains used for WRF and CHIMERE simulations. Nesting configuration on the left. Metropolitan high resolution domain on the right.

Usually, weather and energy uses in winter lead to higher particulate pollution events, due to the combination of a shallow Planetary Boundary Layer and temperature inversions when the ground is cold, and a higher need for heating energy. So far, the day-to-day variability of PM concentrations in the region in winter time is not very well understood, and the capacity of CHIMERE to reproduce PM concentration peaks has not been thoroughly tested yet over South America. Several factors can affect these concentrations such as local production, transport from other places, funneled masses in the valleys... That is why Chilean scientists have conducted several on-site measurement campaigns in winter in the last years, which constitutes a highly valuable database from which we will benefit for our study. Even though specific pollution events may occur during summer time, that can be stronger than in winter (e.g. huge forest fires in early 2017 in Chile), winter air is generally more polluted (except for ozone which concentrations are higher during summer). This can be seen with the example of $PM_{2.5}$ concentrations in Santiago over the year 2016, shown in Figure 14, that features a sharp seasonality in both monthly average (left-hand graph) and maximum (right-hand graph) levels. Thus our study will focus on the months from June to September which correspond to winter time in the Southern hemisphere.

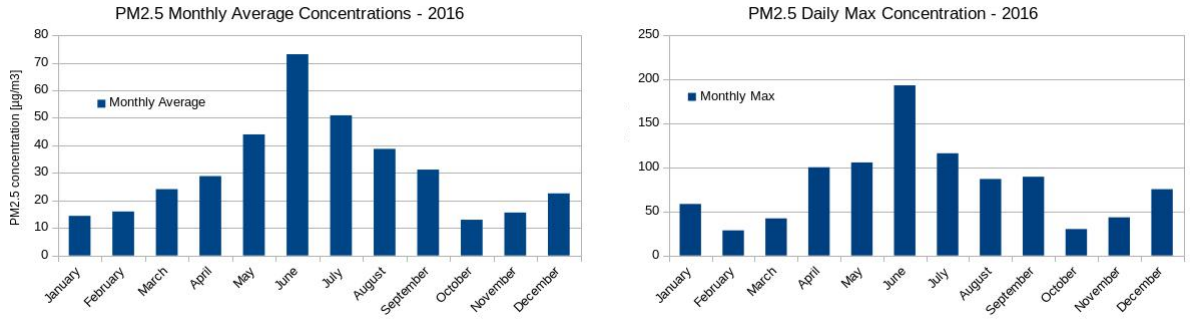


Figure 14: Left: Monthly average $PM_{2.5}$ concentrations (in $\mu g/m^3$) for 2016 over 4 measurement stations in Santiago (El Bosque, Independencia, Pudahuel, Cerro Navia) // Right: Daily maximum by month for the same period/stations - *source* Ministerio del Medio Ambiente.

2.2 Models Used for the Study

As mentioned earlier in Section 1.4, we use the combination of a meteorological model, emissions inventories and a Chemistry-Transport Model (CTM) in order to simulate atmospheric concentrations of pollutants. Let us introduce these three components.

2.2.1 Meteorological Model - WRF

Weather Research and Forecasting (WRF) is a numerical weather prediction system designed for atmospheric simulations (National Center for Atmospheric Research, 2018). Its uses range from research studies to operational forecasting, with a wide variety of scales. The model is developed and maintained by the US National Oceanic and Atmospheric Administration (NOAA) in collaboration with weather agencies all over the world. In this work we use WRF 3.9.1.1 version (Skamarock et al., 2008).

Several studies have been conducted, showing that WRF results are somewhat sensitive to the configuration and parameterization adopted. In particular, Ruiz et al., 2010 focuses on the validation of WRF parameterizations in South America, comparing different schemes outcomes against surface meteorological variables. The results obtained feature a significant variability depending on the modeling approaches. Their findings also include that there is no unique model design that best fits all variables over South America, and that the best performances are given by an ensemble mean - similarly to what is done for the MACC runs in Europe for instance, that average multiple Chemistry-Transport Models results (and thus different configurations). However, our computing power and time being limited, we cannot use ensemble simulations. WRF meteorology is also sensitive to grid resolution, with higher-resolution simulations showing a much improved representation of key meteorological variables (Crippa et al., 2017). That is why a first step of this project is to find an appropriate configuration of WRF that is able to reproduce, on the whole, observed meteorological data (see Section 3.1).

2.2.2 Chemistry-Transport Model - CHIMERE

CHIMERE is an Eulerian off-line (the online version is under development) 3-dimensional Chemistry-Transport Model (CTM), able to reproduce gas-phase chemistry, aerosols formation, transport and deposition. In this study we use the 2017 version of CHIMERE (Mailler et al., 2017). This model is used for research and operational purposes worldwide as can be seen on the map from CHIMERE website (Figure 15). It is also one of the 7 CTMs used for daily European forecasts of Air Quality by the Monitoring Atmospheric Composition and Climate (MACC) EU project (EU Copernicus). As CHIMERE is an off-line model (i.e. does not generate nor has feedback on meteorological conditions), it needs to be provided with meteorological fields from WRF, either interpolated/simulated based on real data or entirely simulated (for future climate studies purposes for instance).

Outputs of CHIMERE include the meteorology fields interpolated from WRF, and the concentrations or mixing ratios of about 50 pollutants. We will mostly focus on a short list of pollutants though, of which

$PM_{2.5}$ and NO_x in particular.

Another limitation of the overall model, on top of WRF sensitivity to parameterization, is that there are specific cases when it appears difficult with an off-line chemistry-transport model to capture pollution peaks. In particular, a recent study by Wang et al. shows that underestimation of PM explosive growth events in models can stem from the absence of aerosols-radiation feedback (this feedback is not available in an off-line model). The region studied by Wang et al. (Beijing-Tianjin-Hebei) is quite different from Santiago in terms of climate and topography, but it suggests that there are cases where online calculation of aerosol-radiation feedback is mandatory to reproduce PM peaks.

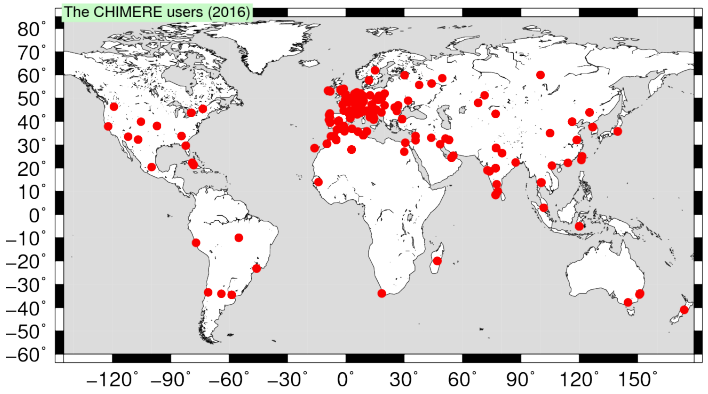


Figure 15: CHIMERE users across the world as of 2016 - *source Laboratoire de Météorologie Dynamique.*

2.2.3 Anthropogenic Emissions Model - EDGAR-HTAP

Several publicly available databases for air pollutants emissions inventories can be used for research purposes. The two major ones used at LMD are EMEP (European Monitoring and Evaluation Programme) and HTAP (Hemispheric Transport Air Pollution) from the EDGAR program (Emissions Database for Global Atmospheric Research). Nevertheless, EMEP covers mainly Europe, and has no data for the South American region we are interested in. That is why we will use HTAP data, similarly to Mazzeo et al., 2018.

The HTAP_V2 dataset consists of 0.1°x0.1° grid-maps of modeled air pollutant emissions for the years 2008 and 2010 (we use the 2010 inventory in the continuation). HTAP uses nationally reported emissions combined with regional scientific inventories in the format of sector-specific grid-maps (8 sectors corresponding to different types of uses of energy) - see Task Force on Hemispheric Transport of Air Pollution. As an illustration of the data available, below are two world maps provided by HTAP, showing NO_x emissions levels from transport and ship sectors in 2010:

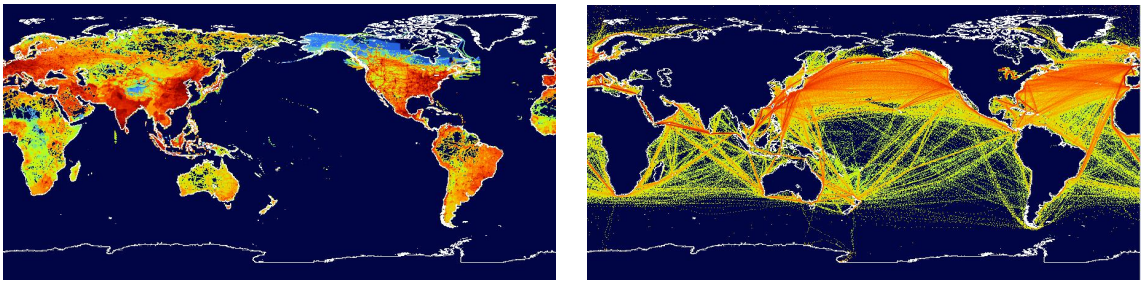


Figure 16: HTAP Worldwide NO_x Emissions Inventories for 2010 for Transport (left) and Ship (right) Sectors.

Given the 0.1° by 0.1° resolution (i.e. roughly 10km by 10km) of this modeled data, we pre-process the raw files from HTAP (downscaling) in order to adapt it to the desired resolution in CHIMERE simulation, depending on land-use characteristics. In addition, HTAP provides monthly inventories, that have to be split in time down to daily/hourly emissions. Despite the fact that HTAP data set applies for 2010 only, we use these emissions levels as representative of the current ones, since no publicly available global

emission inventory has been produced for more recent years. Local missions to build such inventories have been conducted in Chile, but so far their reliability and availability in terms of spatial distribution do not seem satisfactory enough to justify substituting HTAP inventories (Gallardo et al., 2018).

2.2.4 RCP Emission Scenarios

RCP scenario model data is freely available online (IPCC). Data sets are provided with a 0.5°x0.5° grid resolution, containing annual anthropogenic emission rates split by species and sectors of emission, for each projection years considered in the IPCC framework, i.e. every 10 years between 2000 and 2100. Given consistency issues with respect to HTAP data (time scales, resolution, emission levels in 2010...), our analysis of the evolution of air pollution will be based on a comparison between:

- IPCC scenario as of 2000 (only common basis for all the scenarios),
- IPCC RCP2.6 scenario in 2050,
- IPCC RCP8.5 scenario in 2050,

The meteorology used, however, will still be the one simulated and validated for 2016. HTAP emission data will be used for model validation purposes but not taken into account for our projections. After running RCP rough data through a downscaling tool developed at LMD, emission maps obtained for fine Black Carbon (for illustration) are shown in Figure 17.

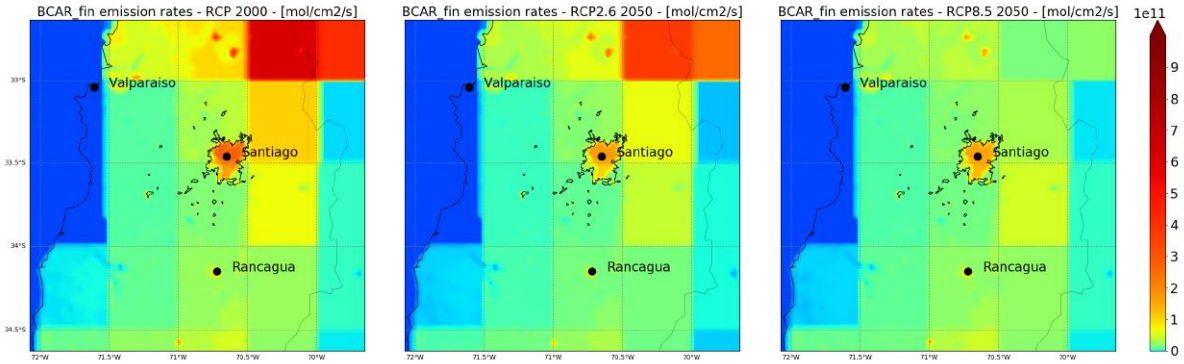


Figure 17: Ground level fine BC emission rates for 2000 (left), 2050 RPC2.6 (middle), 2050 RCP8.5 (right) - after pre-processing.

These maps are consistent with the analysis made in Section 1 on Figure 12: sharp reductions of BC emissions are expected in both scenarios, with a higher decrease under RCP8.5 scenario. This trend is clearly visible for Santiago and for the Northern part of the region. For OC

Scenario parameters consideration

RCP scenarios encompass multiple aspects of future anthropogenic forcing. In addition to pollutants emissions, greenhouse gases emissions and land-use changes are also taken into account to form these representations of climate in the coming years. However, for now, CTM errors induced by approximations on emissions and meteorological fields outweigh potential refined land-use and climate change contributions on simulated pollutants air concentrations (Solazzo et al., 2017). As a first order projection, our methodological choice here is not to take into account possible land-use changes in Santiago by 2050, and to assume that climate has not changed yet, so that winter meteorology in 2050 will remain similar to the weather conditions observed in 2016. Thus, our study consists in replacing current emission levels with projected 2050 emissions, all other things (weather conditions, land-use...) remaining unchanged with respect to 2016. A second step could include a changing climate/land-use in the next studies, but here we still obtain a precious result with the isolated impact of emission schemes on future air quality.

2.3 Model Input Data and Observation Measurements

2.3.1 Land Data

Land-use and topography are key variables to take into account in Chemsitry-Transport Models as they will strongly influence the simulation. Indeed, land-use (whether the land is urban, forest, mountain, desert...) allows to assess what will happen to pollutants emitted or transported over these areas. These geographical characteristics are also used to downscale emissions inventories. Topography allows to assess transport since atmospheric circulation is not constrained the same way over a flat land or in a valley, for instance. The input data used in this study for these two criteria is the Modified IGBP MODIS 20-category land-use database and is shown in Figure 18 below. This database has a 30" resolution (i.e. 0.0083°x0.0083°). Land-use categories provided include:

(1) Evergreen Needleleaf Forest	(2) Evergreen Broadleaf Forest	(3) Deciduous Needleleaf Forest
(4) Deciduous Broadleaf Forest	(5) Mixed Forests	(6) Closed Shrublands
(7) Open Shrublands	(8) Woody Savannas	(9) Savannas
(10) Grasslands	(11) Permanent Wetland	(12) Croplands
(13) Urban and Built-Up	(14) Cropland/Natural Vegetation Mosaic	(15) Snow and Ice
(16) Barren or Sparsely Vegetated	(17) Ocean	(18) Wooded Tundra
(19) Mixed Tundra	(20) Bare Ground Tundra	

In this study, when considering the future of Santiago, we do not take into account potential land-use changes that are likely to appear along the development of the metropolis. Despite a current slow urbanization rate (∼1%) in Santiago, mainly through the sprawl of the outer belts, it is expected that the city will further extend its suburban area in the next decades (Gallardo et al., 2018). However, the main objective of our study is to assess the sensitivity of air pollution in Santiago to future schemes of emissions, all other things being equal.

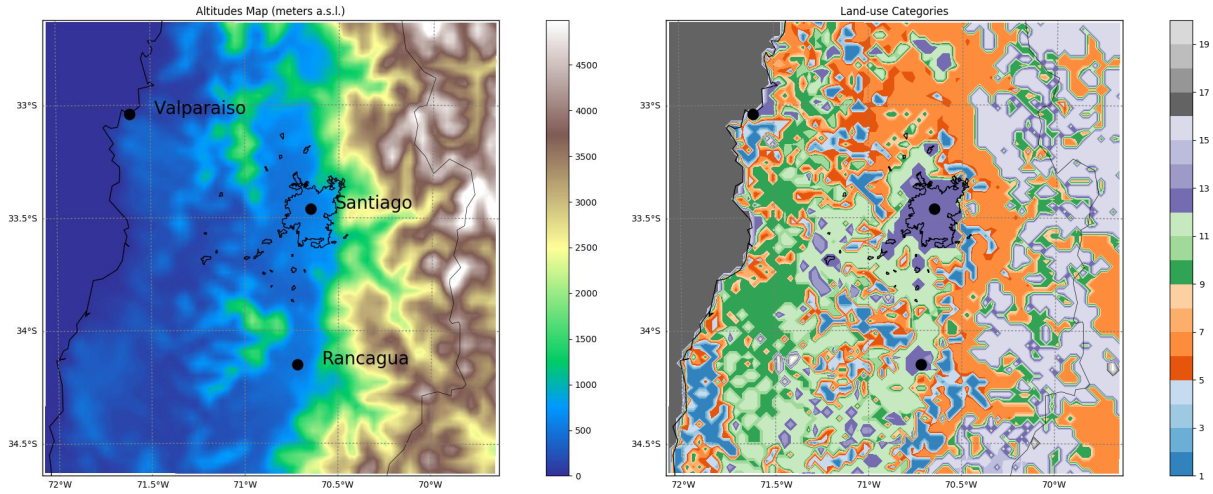


Figure 18: Topography (left) and Land-use (right) input data used in the simulations - source The USGS Land Cover Institute.

2.3.2 *In-situ* Data

Once emissions, meteorology and land properties are fed into CHIMERE, the result of the simulation is a set of 3D-gridded hourly air pollutants concentrations for the time period considered. In order to assess the performance of the model, these results must be compared to local concentration measurements and meteorological data. To do so, several local data sources are used:

- "Sistema de Información Nacional de Calidad del Aire" (SINCA): network of meteorological and air quality sensors distributed in the metropolitan area of Santiago (see Figure 19), providing time series for several pollutants concentrations and meteorological variables. Data available at Ministerio del Medio Ambiente.
- On-site profiles measurement campaigns: tethered balloon measurements carried out on two different sites, during one week in late June, with profiles acquired every three hours for meteorological data

and PM concentrations. Daily vertical profiles of meteorology, taken at 3pm during several days in a row, are also available for another site downtown.

- Time series and vertical profiles of meteorological measurements (relative humidity, 2m temperature, wind speed and wind direction) at a station situated in a valley of the Andean foothills, North-East of Santiago, allowing to assess the performance of the model over complex terrain - station "Yerba Loca" (lat -33.31, lon -70.32).
- A ceilometer (laser-based teledetection instrument) is installed on the roof of the geophysics building of the University of Chile, which provides hourly measurements of optical depths, enabling to compute planetary boundary layer heights.

In future studies and in the context of a short-term air quality forecast system, such a data network might be used for data assimilation purposes as well with the coupled version of CHIMERE. Data assimilation offers the possibility to improve CTM outputs by incorporating near real time actual meteorological and chemical data into the model. As such it is likely to be a field of improvement for CTMs in the next few years (Bocquet et al., 2015).

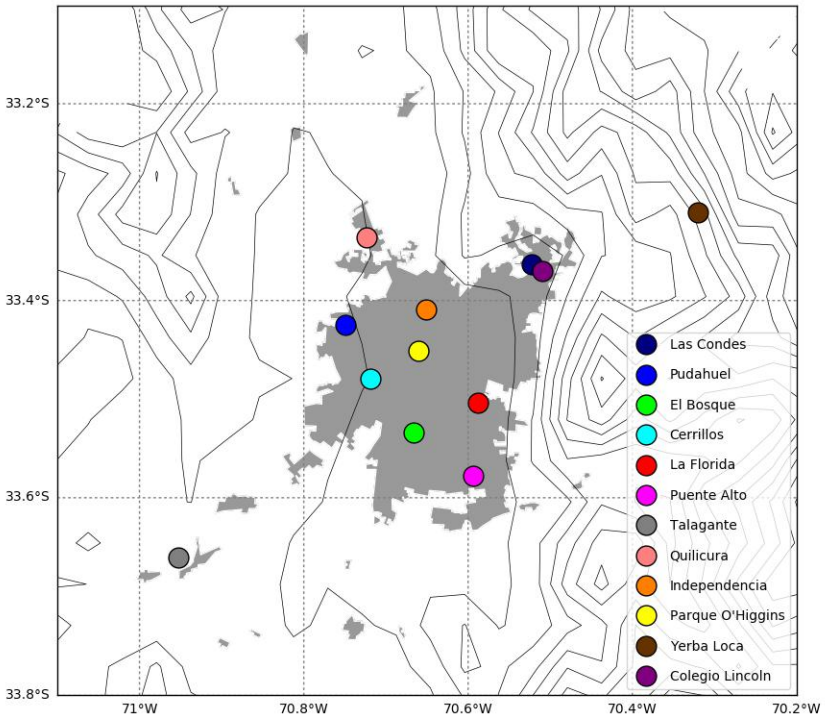


Figure 19: Network of monitors available in Santiago area.

3. Results

In this section we compare on-site observations and CHIMERE simulations on a panel of measurement stations (Figure 19) in order to validate WRF and CHIMERE outputs, and assess the uncertainties linked to these simulations. Then, we present the results obtained for the projected pollutants concentrations in 2050. As a first step aiming to validate our approach for 2050 projected air quality levels, we need to assess the ability of the model configuration to produce consistent results based on a comparison to actual measurements. That is why we run a first simulation on 2016 austral winter in Chile, and compare the results to local measurement data mentioned in the previous section. Then, once the simulation acceptably reproduces observed meteorology and pollutants concentrations in 2016, we can keep the same configuration, substitute emissions, and be confident in the outcomes of the model for 2050.

3.1 Simulated Meteorology - 2016

Three different WRF configurations are tested in order to identify the one that allows to reproduce closely the features of 2016 austral winter meteorology. The main components of these three runs are summarized in Table 1 below. In the continuation we will refer to these three configurations as the "usual European-country configuration" (hereafter UEC), the "adjusted physics configuration" (hereafter APC), and the "adjusted physics + nudging + higher-resolution configuration" (hereafter ANH).

	WRF Configuration		
	UEC	APC	ANH
Nested domain resolution	3km	3km	2km
Coarse domain resolution	15km	15km	10km
Spectral nudging	x=3 / y=5	no	x=3 / y=5
Microphysics	WSM6 (1)	WSM3 (2)	WSM3 (2)
Boundary layer	YSU (3)	MYNN (4)	MYNN (4)
Surface layer	MM5 (5)	MYNN (6)	MYNN (6)
Land surface	Noah LSM (12)	Noah LSM (12)	Noah LSM (12)
Cumulus parameterization	Grell-Freitas (7)	Grell G3 (8)	Grell G3 (8)
Longwave radiation	RRTMG (9)	CAM (10)	CAM (10)
Shortwave radiation	RRTMG (9)	Dudhia (11)	Dudhia (11)
Physical time step	10min		
Chemical time step	5min down to 0.8×CFL constraint		

(1) Hong and Lim, 2006 (2) Hong et al., 2004 (3) Hong et al., 2006
(4) Nakanishi and Niino, 2006 (5) Paulson, 1970 (6) Nakanishi and Niino, 2006
(7) Grell and Freitas, 2013 (8) Grell and Dévényi, 2002 (9) Mlawer et al., 1997
(10) Collins et al., 2004 (11) Dudhia, 1989 (12) Tewari et al., 2004

Table 1: Three WRF configurations evaluated in the study.

Configuration UEC corresponds to the parameterizations usually used at LMD for studies over Euopean regions (France in particular). We wanted to test how it fitted for the very different region of Santiago. Configuration APC corresponds roughly to what is used in Mazzeo et al., 2018 for their study over Chile. Configuration ANH is an attempt at improving configuration APC with a higher-resolution and spectral nudging activation. Because of time constraints the study is limited to these three configurations but in the next steps of the project it will be interesting to assess the performance of other configurations found in the meteorological modeling literature using WRF over Chile (Schmitz and Falvey, 2006 for instance).

In order to determine which configuration performs best, we compute some usual statistical values - mean bias (MB), root mean squared error (RMSE) and Pearson correlation (R) - based on the comparison between observations and simulations over a 5-days period from June 26^{th} midnight to July 1^{st} 2016 midnight (local time) - the time frame is not very extensive due to the use of data from a one-off field measurement campaign. These comparisons are run for the stations "Yerba Loca" and "Colegio Lincoln" (see Figure 19), for which we have both time series and vertical profiles data over the period. The two

stations are situated in locations with very different features. This allows to assess the model performance under varied conditions. Some of these features are introduced below:

- Yerba Loca: this station is situated at the bottom of a valley, along a river, in the cordillera Northeast of Santiago, with surrounding peaks around 400m higher than the valley. Yerba Loca is a National Park and a Nature Sanctuary. Evaluating air pollution in such a place is thus very interesting to study transport of pollutants from Santiago up to the mountains, since very low emissions are expected in this area.
- Colegio Lincoln: contrarily, this station is located in an urban area Northeast Santiago (in Las Condes, a commune of Santiago). This urban area is thus a zone of high emissions of pollutants. In addition, Las Condes is rather flat, which implies significant differences in advection patterns between the two stations, and less resolution constraints than at Yerba Loca. Yerba Loca, Colegio Lincoln and downtown are aligned which is therefore interesting for pollution transport study purposes.

The model vs observations statistics for ground level hourly time series of 2m air temperature (TEMP - in °C), surface air relative humidity (RH - in %) and 10m wind speed (WS - in m/s) are gathered in Table 2. The corresponding graphical representation of these time series is shown in Figure 20. In order to assess the performance of the configuration at the surface level over a longer time period, we compute the same statistics for two automated stations in Santiago from the SINCA network (see Figure 19), between June 15^{th} and July 15^{th}. The results are gathered in Table 3.

	Surface time series statistics						
	Network:	*Yerba Loca*			*Colegio Lincoln*		
Configuration UEC		MB	RMSE	R	MB	RMSE	R
	TEMP	-2.0	2.93	0.90	3.03	4.20	0.82
	RH	-5.52	15.48	0.69	-24.13	30.71	0.51
	WS	2.38	3.55	0.08	0.39	0.55	0.42
Configuration APC		MB	RMSE	R	MB	RMSE	R
	TEMP	-3.66	4.92	0.69	-0.42	2.19	0.89
	RH	1.75	21.19	0.36	-17.37	23.91	0.64
	WS	3.93	7.7	-0.21	-0.22	0.34	0.13
Configuration ANH		MB	RMSE	R	MB	RMSE	R
	TEMP	-4.87	5.27	0.87	-1.62	2.45	0.92
	RH	-5.25	17.52	0.45	-19.91	25.03	0.69
	WS	0.72	2.78	-0.37	-0.04	0.27	0.11

NB: 10m wind speeds are 6-hour averages.

Table 2: Statistics comparing observed and simulated meteorological **time series** for 3 configurations of WRF for 2 stations in Santiago.

Generally speaking, the model is able to reproduce diurnal cycles, shows appropriate magnitudes and captures deviations for temperature, humidity and wind:

- Temperature: configuration UEC features good correlation levels at both sites but significant biases of -2°C at Yerba Loca and +3°C at Colegio Lincoln. Configurations APC and ANH perform less well at Yerba Loca but show very good characteristics at Colegio Lincoln site with small biases and very high correlations (0.89 and 0.92 respectively). As for the two SINCA sites that are over flatter areas, APC and ANH perform quite well, with once again high correlations and small biases, while UEC does not seem to be a very appropriate configuration.

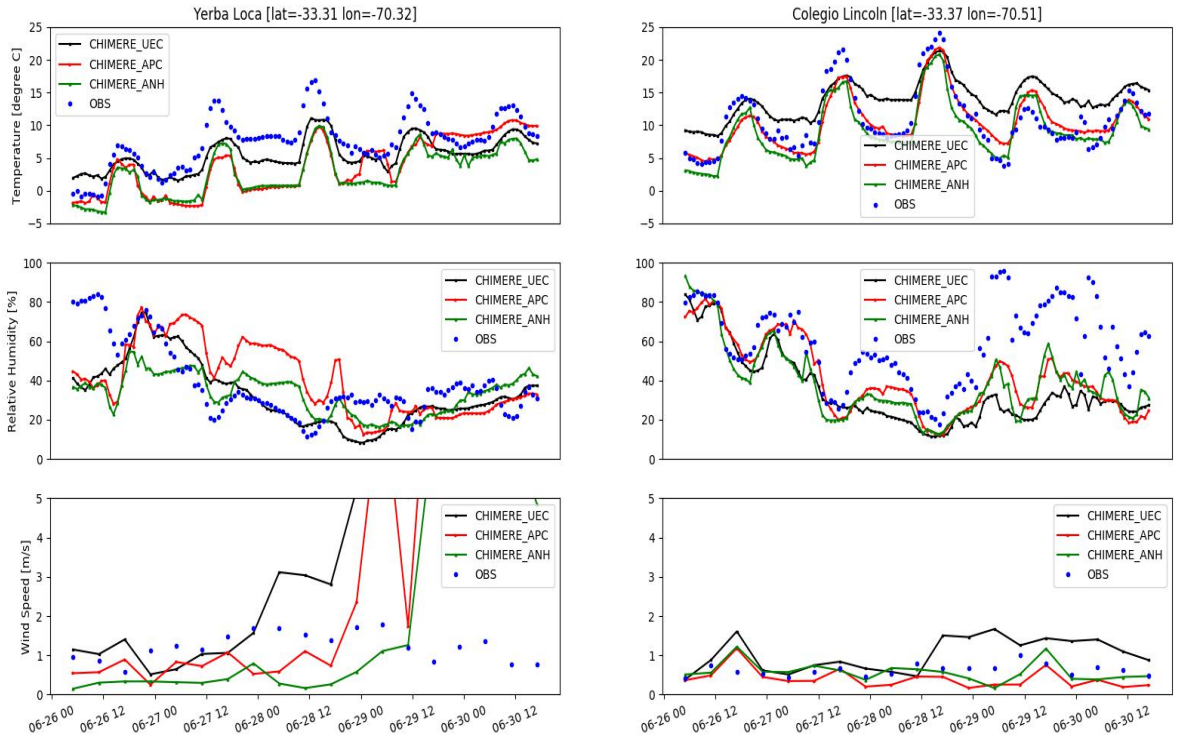


Figure 20: Observed (blue dots) and simulated (lines) time series for temperature (top), relative humidity (middle) and wind speed (bottom), for Yerba Loca (left) and Colegio Lincoln (right) stations.

	Surface time series statistics						
	Network:	*El Bosque*			*Talagante*		
UEC		MB	RMSE	R	MB	RMSE	R
	TEMP	4.99	5.88	0.74 :	4.56	5.36	0.76
	RH	-27.34	31.7	0.55 :	-28.09	33.7	0.42
	WS	0.33	0.63	0.41 :	1.06	1.3	0.3
APC		MB	RMSE	R	MB	RMSE	R
	TEMP	1.51	2.94	0.84 :	-0.18	2.54	0.82
	RH	-14.16	22.48	0.62 :	-4.33	20.66	0.54
	WS	-0.1	0.41	0.46 :	0.6	0.9	0.52
ANH		MB	RMSE	R	MB	RMSE	R
	TEMP	1.23	2.83	0.84 :	1.73	3.38	0.74
	RH	-14.85	23.44	0.60 :	-17.45	24.2	0.48
	WS	-0.14	0.43	0.33 :	0.67	0.93	0.46

NB: 10m wind speeds are 6-hour averages.

Table 3: Statistics comparing observed and simulated meteorological **time series** for 3 configurations of WRF and for 2 SINCA stations in Santiago.

- Relative Humidity: the compared performances of the models are the same as for temperature generally speaking (i.e. UEC performs less bad at Yerba Loca but APC and ANH behave clearly better at the three other sites) although the correlations are smaller and biases much higher. On the whole, except for Yerba Loca, the model is significantly dryer than what is observed. This too small relative humidity can lead to underestimation of secondary aerosols nucleation (sulfuric acid nucleation in water for instance), that occurs when a trace gas in the atmosphere condensates and becomes a solid/liquid particle. This is a major source of fine particles (Villalobos et al., 2015) so that its underestimation can be quite damaging.

- Wind Speed: for the Yerba Loca site, all the models identify a sharp increase of wind speeds, that reach very high values at the end of the period. This does not appear in the observations. So far we were not able to explain this phenomenon which leaves room for further analysis in the continuation of the project. A hypothesis could be that the coastal low event observed in June 2016 could actually lead to such high wind velocities in the area of Yerba Loca, but they do not appear at the measurement site which is in the valley. The model's resolution would then be to blame here but not its simulated components. This still has to be investigated. However at the two SINCA sites, configurations APC and ANH demonstrate good estimations of 6h average wind speeds, with decent correlation and reasonable biases, which is not the case with UEC configuration.

This first time series analysis over meteorological values seems to eliminate configuration UEC that does not perform well at reproducing observed meteorology. In addition, the two other configurations show very promising features for the continuation.

The same statistical values can be computed to assess the consistency between observed and simulated vertical profiles (see Table 4). We are not sure about the reliability of the vertical profiles measured at Yerba Loca and Colegio Lincoln sites. Weird profile shapes in the data cannot explained. As a result we show here the profiles for the station "DMC" which is located downtown [33.43°S, 70.68°W] only. These profiles are assessed on June 27^{th}, 28^{th} and 29^{th} 2016 at 3pm UTC, based on data availability and interest of these particular dates that featured peaks of PM pollution in Santiago. The corresponding graphical representation of these vertical profiles is shown in Figure 21. Given Table 4 and Figure 21, it seems that configuration UEC still performs less well than the others for vertical profiles, especially considering June 29^{th}. On the whole, the model is able to produce reasonable vertical profiles with the following limitations:

- Although temperature profiles on the first two days are very good, the last day is much hotter than observed and does not capture the strong inversion observed around 500 a.g.l. which might lead to underestimations of pollutants concentrations. However, the observed inversion layers are well reproduced by the models on each day, which is a very important prerequisite in order to have correct pollution estimations.

- As for relative humidity, the models are too dry in the lower layers but behave fairly well higher up, with the same consequences on chemistry as mentioned previously. It is worth mentioning that the very dry atmospheres of June 28^{th} and 29^{th} are well captured by the model. As is the case for the wetter conditions of June 27^{th} that are probably linked to high altitude clouds presence on that day.

- Wind profiles show appropriate magnitudes and shapes near the ground although they show some differences with observations in the free troposphere. Local scale transport should be satisfactory though, depending on wind direction.

As for the ability of the models to reproduce PBLH, we show in Figure 22 the comparison between ceilometer data measured and modeled at the Department of Geophysics - Universidad de Chile [33.46°S, 70.66°W]. Ceilometer data shows daytime PBLH that can reach up to 400m to 700m around midday. The models capture good magnitudes for boundary layer heights on the whole period and reproduce a clear diurnal cycle. With configuration UEC, the model is not able to resolve PBLH at night and thus sets it to 23m each night. Configurations APC and ANH simulate around 100m at night which seems reasonable although we do not have meaningful data from the ceilometer during nights. However, they differ on their diurnal cycles where ANH tends to underestimate PBLH during day time. Thus, the best configuration for PBLH estimation seems to be APC.

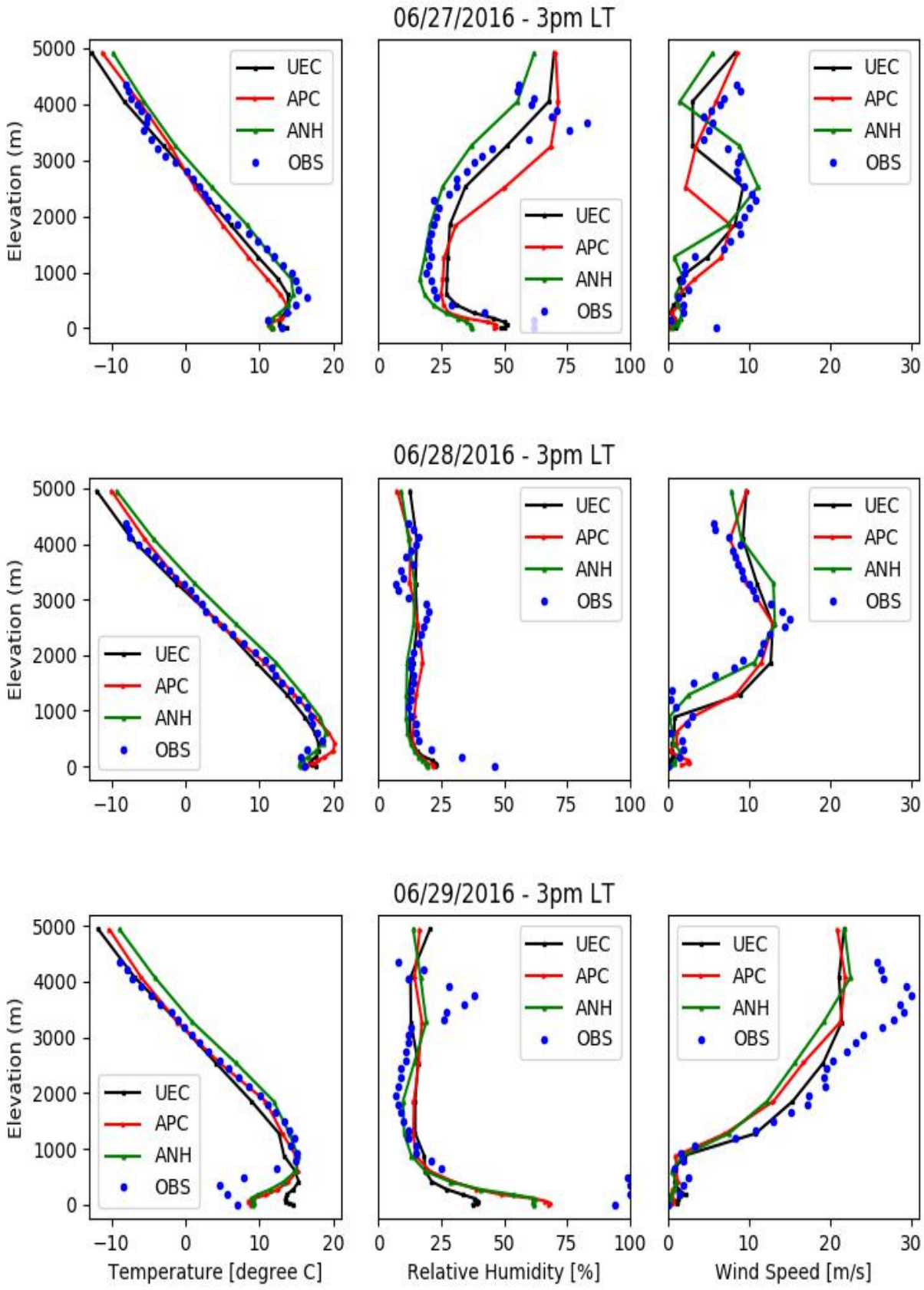


Figure 21: Observed (blue dots) and simulated (lines) vertical profiles for temperature (left), relative humidity (center) and wind speed (right), for June 27^{th} (top), 28^{th} (middle) and 29^{th} (bottom) at DMC site.

Vertical profiles statistics - DMC site											
	June 27^{th} 2016				June 28^{th} 2016				June 29^{th} 2016		
UEC	MB	RMSE	R		MB	RMSE	R		MB	RMSE	R
TEMP	-0.75	1.38	0.99	:	-0.44	0.9	1.0	:	0.51	3.28	0.91
RH	2.32	9.16	0.91	:	-1.1	5.8	0.77	:	-10.2	27.04	0.78
WS	-1.62	2.3	0.85	:	1.52	3.08	0.82	:	-2.48	3.92	0.98
APC	MB	RMSE	R		MB	RMSE	R		MB	RMSE	R
TEMP	-0.79	2.01	0.99	:	0.51	1.1	0.99	:	0.83	2.4	0.95
RH	7.64	14.3	0.80	:	-1.04	5.88	0.67	:	-7.47	22.2	0.82
WS	-1.92	3.54	0.39	:	1.06	2.71	0.84	:	-3.63	4.38	0.99
ANH	MB	RMSE	R		MB	RMSE	R		MB	RMSE	R
TEMP	0.85	1.52	0.99	:	1.6	1.75	1.0	:	2.02	2.68	0.97
RH	-8.45	13.22	0.88	:	-2.73	6.56	0.68	:	-8.46	22.08	0.85
WS	-1.16	2.71	0.74	:	0.96	1.91	0.94	:	-4.1	5.01	0.99

Table 4: Statistics comparing observed and simulated meteorological **vertical profiles** for 3 configurations of WRF and for 3 days at DMC station in Santiago.

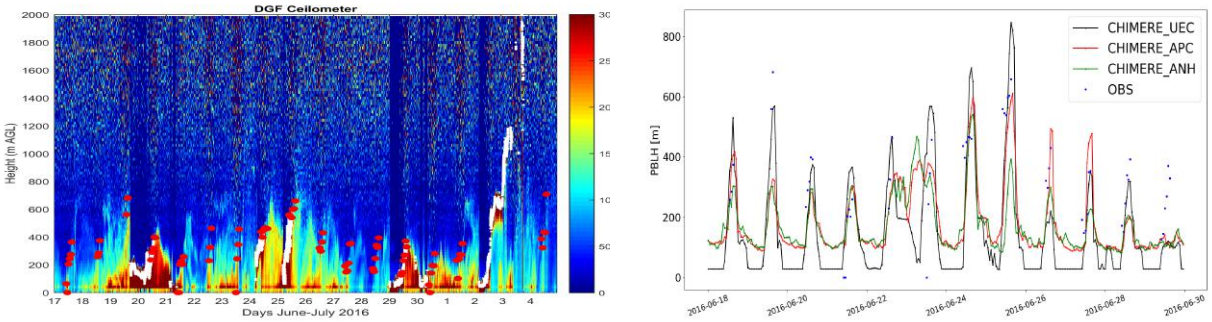


Figure 22: Planetary Boundary Layer Heights measured via ceilometer at the University of Chile (left) and comparison with the simulated PBLH (right).

Based on the analyses performed in this section, configurations APC and ANH are good candidates to be kept for the continuation. Because of the time constraints of the project, and the occurrence of some numerical stability issues with configuration ANH, we decide to keep **configuration "APC"** for the continuation. The gain we would obtain in terms of resolution with ANH does not provide significant improvements in the meteorology but doubles runtime, with simulations lasting more than 10 days to cover only 45 days. As for pollutionn, ANH does not perform really better either, with a very small reduction of the bias on NO_x on some stations but no improvement in terms of correlation. As for $PM_{2.5}$, then again ANH is not significantly better than APC and even introduces a strong positive bias for several measurement stations, but does not allow to account for peak events. This counter-intuitive lack of improvement under higher resolution must be further investigated in the continuation of the project.

3.2 Simulated Concentrations - 2016

Now that we have a satisfactory meteorological configuration, we need to assess the ability of the model to reproduce observed pollutants concentrations. Then again we compute mean bias, RMSE and correlation for the concentrations of $PM_{2.5}$ (in $\mu g/m^3$) and NO_x (in ppb), for six automated stations

Network:	*El Bosque*				*Las Condes*				*Pudahuel*		
	MB	RMSE	R	:	MB	RMSE	R	:	MB	RMSE	R
$PM_{2.5}$	-20.06	63.95	0.27	:	8.18	23.05	0.65	:	-6.28	75.41	0.12
NO_x	-130.4	172.4	0.41	:	-53.57	71.12	0.47	:	-43.04	128.5	0.28
	La Florida				*Puente Alto*				*Parque O'Higgins*		
	MB	RMSE	R	:	MB	RMSE	R	:	MB	RMSE	R
$PM_{2.5}$	-0.58	33.2	0.47	:	-7.09	33.49	0.47	:	14.09	40.77	0.44
NO_x	-110.5	144.9	0.37	:	-75.62	100.5	0.52	:	-86.39	129.7	0.43

Table 5: Statistics comparing observed and simulated pollutants concentrations **time series** for 6 stations in Santiago - $PM_{2.5}$ in [$\mu g/m^3$] and NO_x in [ppb].

in Santiago from the SINCA network (see Figure 19), between June 15^{th} and July 15^{th}. The results are gathered in Table 5. The model reproduces fairly well mean levels of $PM_{2.5}$ concentrations, with a particularly high time correlation and small bias at stations where there are no peak events over the period (Las Condes site for instance shows a bias smaller than $10\mu g/m^3$ and a correlation of 0.65 over a long time period). However, the model is not able yet to account for the two sharp peaks of $PM_{2.5}$ observed in late June (see Figure 23), and does not perform very well for highly polluted sites such as El Bosque and Pudahuel that show the highest levels of $PM_{2.5}$ concentrations over the time series considered. We can see on Figures 20 and 21 though that meteorology on June 27^{th}, day of the second sharp $PM_{2.5}$ peak, is quite well reproduced both at the surface level and vertically for downtown stations. As a consequence we can probably attribute this underestimation to the fact that the source emissions inventories we use are monthly and static as of 2010, which does not allow to capture exceptional peaks of emissions. These events seem indeed local since the wealthy neighborhood of Las Condes for example does not show this pollution peak although the meteorological conditions are not very different from the other sites in Santiago. In addition, it is possible that the lack of aerosol feedback on meteorology in this version of CHIMERE also accounts for a part of concentrations underestimation during these peaks (see Wang et al., 2018 for instance). As a result, using the coupled WRF-CHIMERE model currently under development will be of great interest for the continuation of the project in order to assess its capacity to capture pollution events. On the other hand, the model sometimes overestimates $PM_{2.5}$ concentrations, the best example being on June 29^{th} (see Figure 23). This can be traced back to the significant underestimation of the PBLH on that day where observations show a PBLH reaching up to 400m while the model does not get higher than 200m (see Figure 22). The same explanation applies for June 20^{th}.

As for NO_x the model significantly underestimates mixing ratios at all stations and for the whole period (Figure 24). The huge negative bias obtained on every station is not satisfactory. Mazzeo et al., 2018 also find a negative bias on NO_x but way less important. However in their study they use a more accurate emissions inventory on Santiago for 2015, featuring much higher emission levels than those given by HTAP. This probably accounts better for actual NO_x emissions, enabling to reproduce more closely observed NO_x pollution. Thus, the limitation of our model here is likely the lack of accuracy of our emissions inventory since the temporal correlations we obtain, far from being extraordinary still show decent values despite too low emissions in input. Similarly to $PM_{2.5}$ the most polluted sites of El Bosque and Pudahuel are less well reproduced by the model.

Generally speaking, when considering the figures in Table 5, one needs to remind that the statistics are significantly affected by the occurrence of pollution peaks. Over a shorter time period without peak events, the statistics obtained are much better, closer to the ones shown at Las Condes for instance.

In Figure 25 we show the spatial repartition of concentrations simulated by the model and observed in the SINCA network. These values are 6-hour averages. The concentration bins used on these maps correspond to the official daily average concentration thresholds of $PM_{2.5}$ as defined by the Chilean environmental regulation ('Good', 'Regular', 'Alert', 'Pre-Emergency', 'Emergency') - Ministerio del Medio Ambiente, 2012. We can see that the model simulates adequate spatial repartition of pollutants over the area along the two days shown here. At some points the model and observations do not give the same alert level, but there are very few cases when the two levels differ by more than one step. A satisfactory feature on the

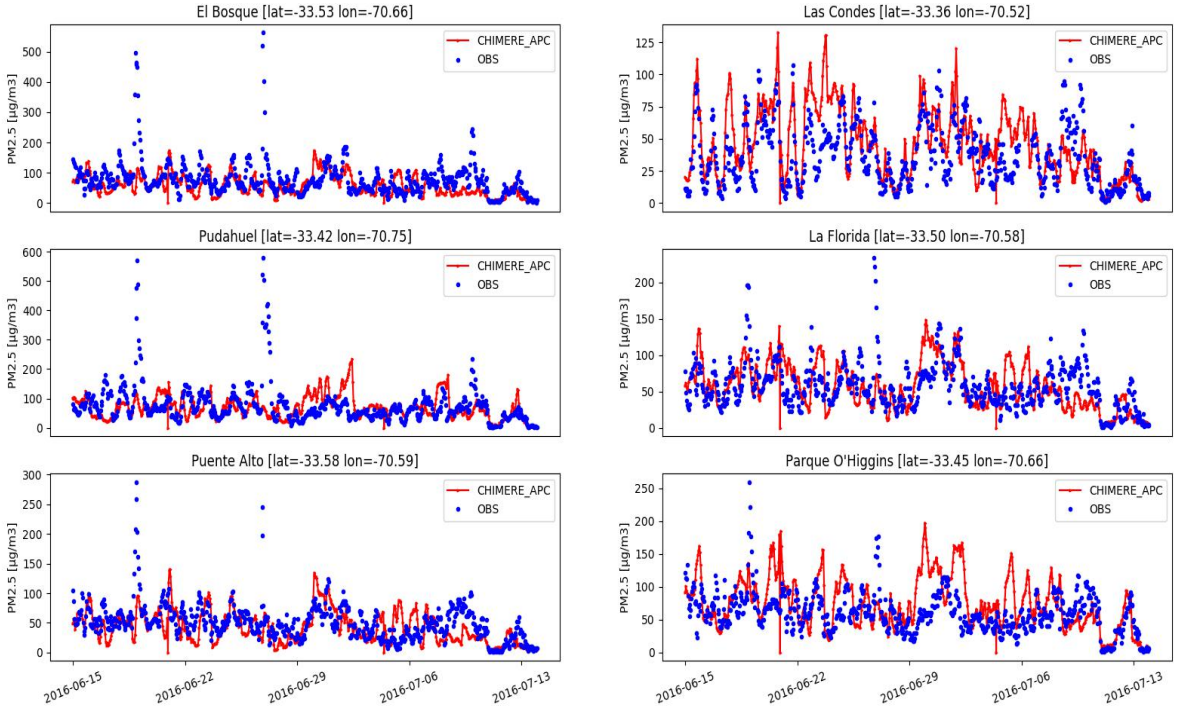


Figure 23: Observed (blue dots) and simulated (lines) time series for $PM_{2.5}$ concentration for 6 stations in Santiago.

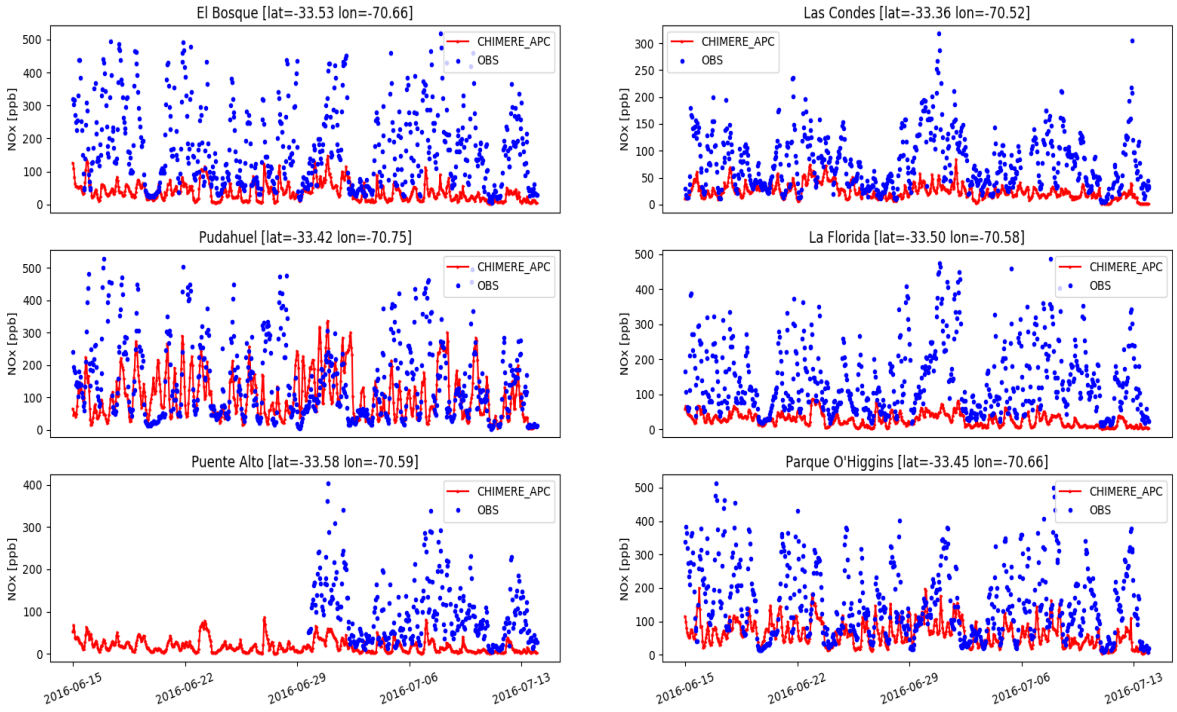


Figure 24: Observed (blue dots) and simulated (lines) time series for NO_x mixing ratio for 6 stations in Santiago.

spatial repartition we obtain is that its daily pattern matches the one described in Airparif, 2006, featuring pollution masses present in Western Santiago in the morning and transported towards the Eastern part of the city in the afternoon. Although it cannot be seen on these 6-hour averages, it comes very clear on hourly animated maps from our CHIMERE simulations.

For a better quantitative analysis of the ability of the model to simulate adequately alert thresholds, we build a matrix showing the correlations between simulated and observed episodes, over one month between June 15^{th} and July 15^{th} 2016 (Table 6). We use the same thresholds as defined above. We include all the SINCA stations of the metropolitan area as well as Rancagua, Valparaíso and Viña del Mar stations. In this matrix, each cell gathers the count of occurrences (stations and time steps) when the simulated and observed daily average concentrations of $PM_{2.5}$ compare a given way. For instance, the top left cell counts each time and each station when the modeled and observed $PM_{2.5}$ concentration show simultaneously a 'Good' alert level. On the contrary, the bottom left cell gives the number of times and stations for which the observed value gives a 'Good' level of $PM_{2.5}$ while the model sees an 'Emergency' case. From this matrix we find that:

- When the measured level is 'Good', the model simulates a 'Good' event in more than 60% of the cases and foresees an 'Alert' or higher level in only 15% of the cases.
- The model appropriately reproduces the 'Regular' level in 50% of the cases and is off by more than one step in only 6% of the cases.
- Beyond the 'Regular' level, the model has a tendency to underestimate daily $PM_{2.5}$ concentrations. This is consistent with the mainly negative biases seen previously in Table 5.

		Observed				
		Good	*Regular*	*Alert*	*Pre-Emergency*	*Emergency*
Modeled	*Good*	114	42	14	4	2
	Regular	47	66	26	10	0
	Alert	19	17	12	6	0
	Pre-Emergency	8	8	3	0	0
	Emergency	0	0	0	0	0

Table 6: Correlation matrix between observed and modeled $PM_{2.5}$ episodes.

We have shown that the model is able to capture decently variations and deviations of pollutants concentrations despite a strong negative bias on NO_x that we do not fully explain yet except for the inaccuracy of our emission inventory. As for $PM_{2.5}$ the simulations give very good results apart from peak events reproduction. We have to bear this in mind for the 2050 projections described hereafter.

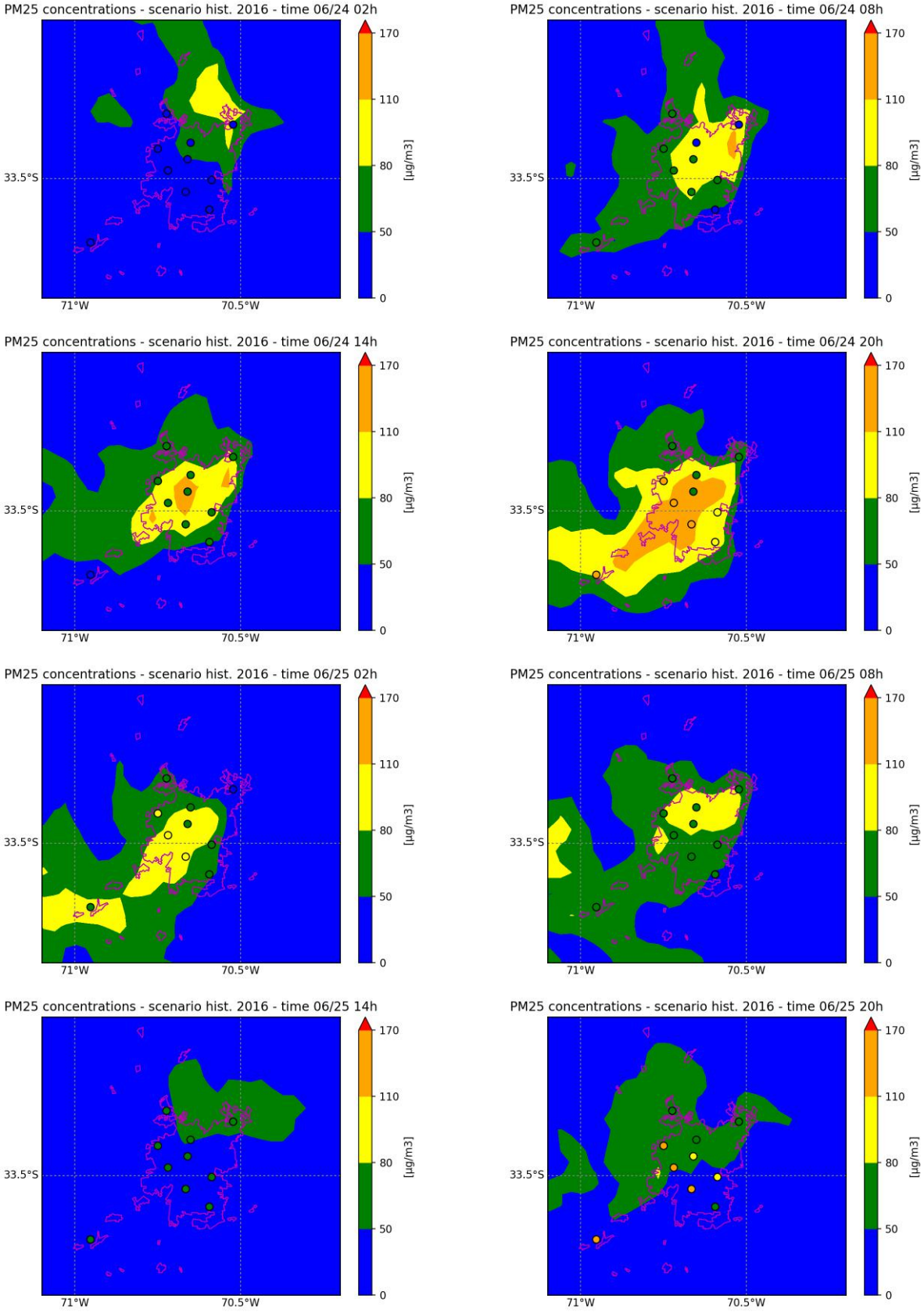


Figure 25: Simulated maps of $PM_{2.5}$ 6-hourly concentrations in Santiago area - colored dots show observed values. Values over 2 whole days (June 24^{th} and 25^{th}) every 6 hours.

3.3 Simulated Concentrations - 2050

Consistently with what is described in the methodology section, the following results are issued from a CHIMERE run with WRF configuration APC described above, substituting 2010 HTAP emissions used for validation by RCP 2000 inventory and projected emissions in RCP8.5 and RCP2.6 scenarios (see Section 2). As mentioned earlier, the station Parque O'Higgins can be considered representative of Santiago's air quality. In Table 7 are gathered average, maximum and standard deviation of $PM_{2.5}$ and NO_x concentrations at Parque O'Higgins over a month (same time period as defined for Table 5) in the three scenarios. Table 8 shows average and maximum $PM_{2.5}$ and NO_x concentrations for a wider region around Santiago defined as [33.9°S,71.1°SW] to [33.1°S,70.3°W]. We can see from these tables that relatively to 2000 both scenarios lead to a decrease in average levels of both pollutants.

	$PM_{2.5}$ [$\mu g/m^3$]				NO_x [ppb]		
Scenario	AVG	MAX	STD		AVG	MAX	STD
2000 RCP	26.94	74.55	14.33	:	10.50	32.30	6.37
2050 RCP8.5	25.26	70.07	14.04	:	8.70	27.22	5.15
2050 RCP2.6	19.04	47.36	9.44	:	2.28	5.92	1.05

Table 7: Average, maximum and standard deviation concentrations of NO_x and $PM_{2.5}$ in the three scenarios - station Parque O'Higgins.

	$PM_{2.5}$ [$\mu g/m^3$]			NO_x [ppb]	
Scenario	AVG	MAX		AVG	MAX
2000 RCP	8.44	81.81	:	2.55	42.98
2050 RCP8.5	7.86	79.97	:	2.13	38.30
2050 RCP2.6	6.84	53.15	:	0.90	7.07

Table 8: Average, maximum and standard deviation concentrations of NO_x and $PM_{2.5}$ in the three scenarios - Metropolitan Area.

$PM_{2.5}$

RCP2.6 scenario leads to a decrease of $PM_{2.5}$ average concentration by 7.9$\mu g/m^3$ i.e. -29%. The maximum simulated concentration also decreases by the same magnitude. The amplitude between lows and highs is tighter than in 2000. RCP8.5 on the other hand is closer to 2000 and leads to a decrease of $PM_{2.5}$ average level by only 1.7$\mu g/m^3$ i.e. -6%. Maximum value and deviation are similar to 2000. As for the metropolitan area, the trends are the same, with an average decrease of 1.6$\mu g/m^3$ i.e. 19% in RCP2.6 scenario and a decrease of 0.58$\mu g/m^3$ i.e. 6%. The distribution of this evolution split by species forming $PM_{2.5}$ is shown in Figure 28. We can see that the decrease in both scenarios is linked to Organic Carbon concentrations falling quite sharply. Although BC falls more in RCP8.5 than RCP2.6 as expected, OC decreases less, and other species like Ammonia (NH_3) and Nitric acid (HNO_3) increase more than BC decreases. In RPC2.6, Sulfuric acid (H_2SO_4) increase is compensated by an equivalent Nitric acid decrease. That is why, in the end, RCP2.6 scenario leads to very good improvements in $PM_{2.5}$ concentrations, while RCP8.5 improvement is rather modest. Spatially speaking, Figure 26 shows that the major reductions in concentrations take place in the Northern region and downtown Santiago. The reduction over Santiago and Rancagua is much clearer in RCP2.6 than RCP8.5, while RCP8.5 features greater reductions in the Northern area than RCP2.6.

NO_x

Despite our model being not completely reliable for NO_x , we can say the following on variations in the two scenarios. As expected given Figure 12, RCP2.6 scenario implies very high reductions in NO_x mixing ratios, while RCP8.5 is moderate. RCP8.5 decreases average levels by roughly 20% at Parque O'Higgins station and over the metropolitan area. RCP2.6 goes far beyond, with reductions of 78% at Parque station

and 65% over the metropolitan area. As for the spatial distribution, the evolution is similar to what is observed for $PM_{2.5}$. Because of the high uncertainties shown by our NO_x modeling, absolute value drops in NO_x mixing ratio cannot be used as results as such since these variations lie way within our confidence intervals. However, the comparison between the scenarios still holds, showing that RCP8.5 leads to a smaller decrease than RCP2.6.

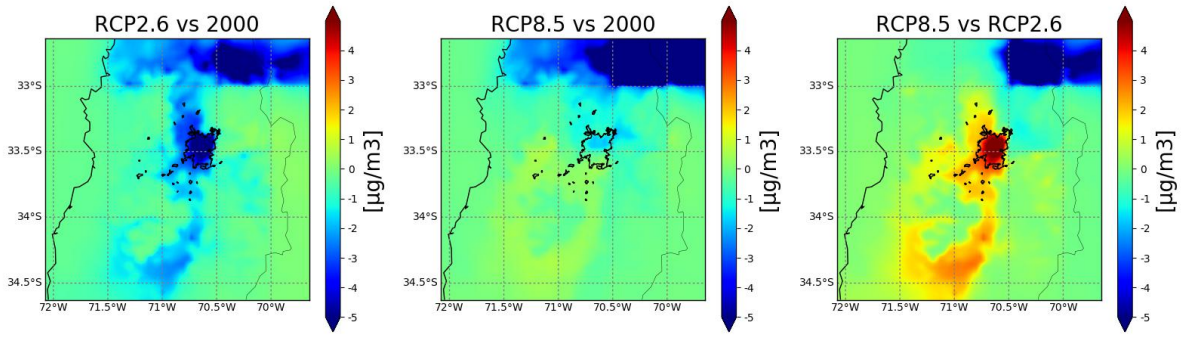


Figure 26: Spatial Comparative Evolution of $PM_{2.5}$ Concentrations - Average over a month between June 15^{th} and July 15^{th}.

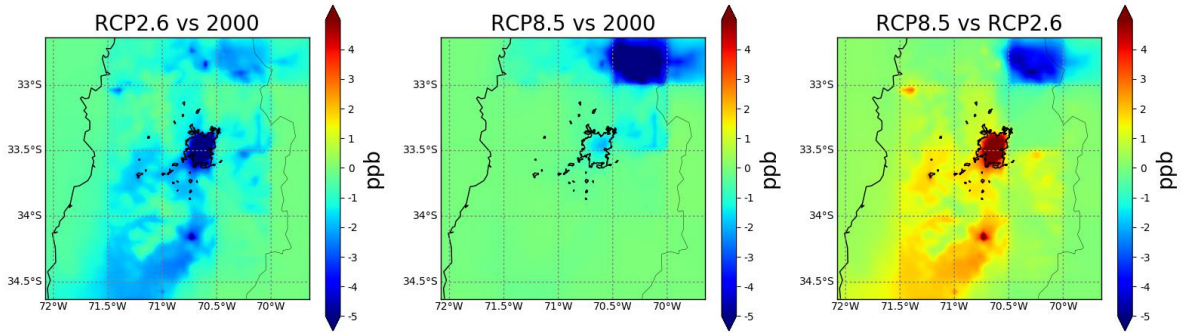


Figure 27: Spatial Comparative Evolution of NO_x Concentrations - Average over a month between June 15^{th} and July 15^{th}.

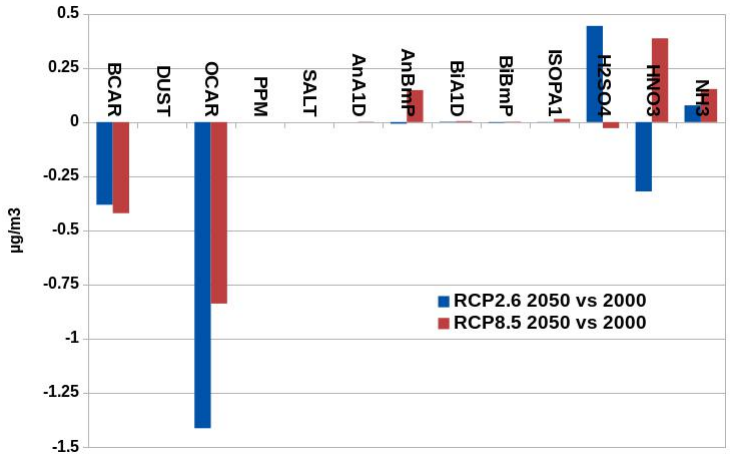


Figure 28: $PM_{2.5}$ components concentration variation in RCP2.6 and RCP8.5 with respect to 2000 - average over Santiago area.

Comparison with HTAP simulation

Figure 29 shows a comparison between the distributions of concentrations in Santiago area in the three RCP scenarios and HTAP simulation run for the model validation. All RCP simulations show very small concentrations compared to our HTAP run. Figures 30 and 31 show much higher emission levels for HTAP than RCP 2000 for H2SO4 (a main contributor to $PM_{2.5}$) and NO_x which explains part of the huge discrepancies. However RCP 2010 emission levels do not match HTAP inventory and remain very low compared to it. HTAP and RCP are not consistent so a comparison is not relevant.

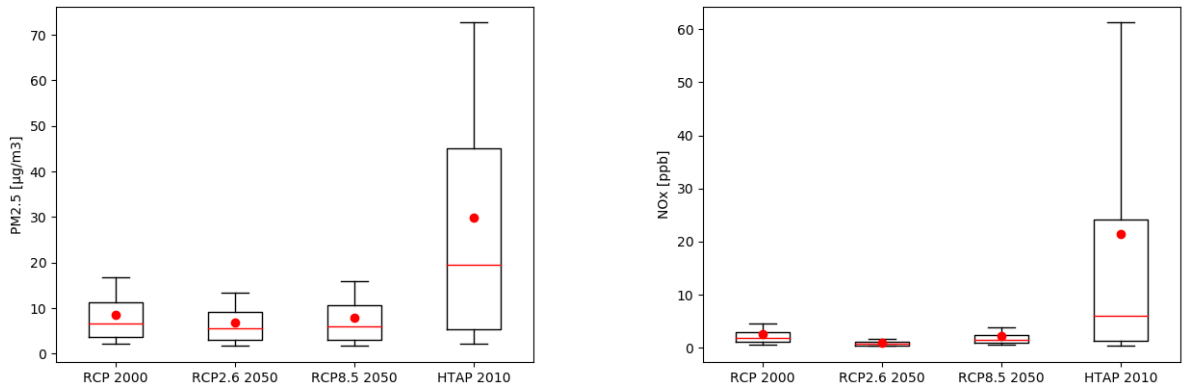


Figure 29: Distribution of $PM_{2.5}$ and NO_x concentrations for 2000, RCP2.6 and RCP8.5 2050 in Santiago area. Boxes indicate the interquartile range, whiskers indicate the first and last decile, lines and circles, respectively indicate medians and means.

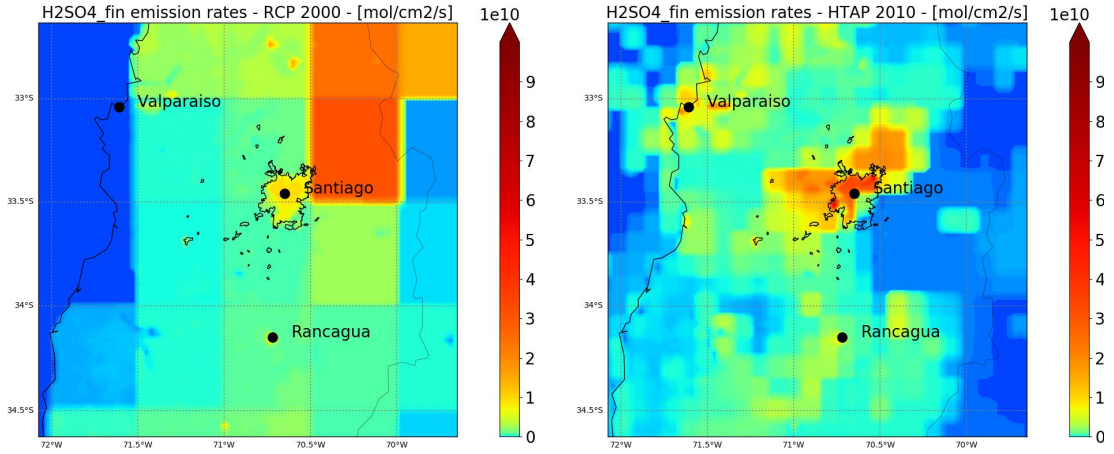


Figure 30: Ground level fine H2SO4 emission rates for 2000 (left) and HTAP 2010 (right) - after pre-processing.

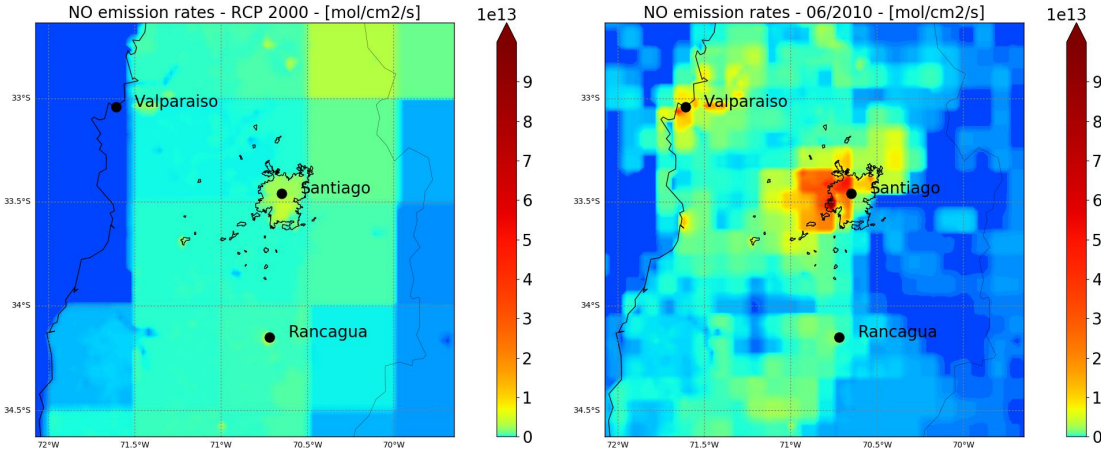


Figure 31: Ground level NO emission rates for 2000 (left) and HTAP 2010 (right) - after pre-processing.

4. Conclusion

Summary

In this study we have shown that despite the challenge induced by a sharp topography of the region, we were able to reproduce past meteorological conditions quite satisfactorily with configuration "APC", except for the mountain site of Yerba Loca, which deserves deeper digging in order to identify the factors that prevent the model from reproducing adequately the meteorology. Average levels and trends of $PM_{2.5}$ concentrations have been quite fairly reproduced. However NO_x simulated levels are not satisfactory yet. Peak events remain very difficult to catch, and their study is likely to benefit from the coupled WRF-CHIMERE model currently under development.

As for the future of air quality in Santiago at the 2050 horizon, our main findings include:

- RCP2.6 implies sharp decreases in 2050 average $PM_{2.5}$ concentrations with respect to 2000, both in Santiago (-7.9$\mu g/m^3$) and in the broader area (-1.6$\mu g/m^3$). RCP8.5 also features decreases on average, but to a much lesser extent (-1.7$\mu g/m^3$ and -0.58$\mu g/m^3$, respectively).
- These variations mainly concern Santiago and the Northern part of the area. The rest of the area does not show a significant sensitivity to the scenarios. $PM_{2.5}$ and NO_x spatial patterns show a similar evolution in both scenarios.
- As mentioned in Section 1, RCP2.6 scenario focuses on GHG mitigation, without dedicated air quality policies, while RCP8.5 takes account of such policies. However, we find that RCP2.6 is still better than RCP8.5 for future air quality. As a result, we may conclude that the co-benefits of a constraining GHG policy are higher than the ones obtained with an air quality focused policy discarding GHG concerns.

Concluding remarks

- A limitation to our results lies in the fact that our validation is made on 2016, with HTAP emission inventories, while RCP projections feature the years 2000 and 2050, and are not necessarily consistent with HTAP. However, we could not reach a better trade-off. We first wanted to compare 2016 and 2050 levels, but any methodology we could think of to do so proved irrelevant because of consistency issues between HTAP and RCP inventories. What's more, RCP scenarios start in 2000 which is the only common basis for all RCP scenarios. In particular, we saw that 2010 levels are very different, so that a baseline comparison with HTAP would have been impossible. A solution would have been to work directly on validating the model as of 2000 using RCP emissions, but validation data for such a period (in particular for meteorology) is quite difficult to obtain given the lesser extent of the measurement network in Santiago at that time. Most SINCA stations comprise meteorological measurement only back to 2003.
- The high-resolution configuration "ANH" showed lots of instabilities during the runs. Several times the output files contained absurd values which implied that the run failed and had to be restarted. Because of this issue, the results of the project were delayed by almost three weeks. So far, we have not been able to identify the very source of this problem. Given that configuration "APC" worked well without showing such instabilities, three main options are considered: either the issue is directly linked to the high-resolution creating sharp gradients that lead to absurd values, or there were some unidentified problems in the development version of CHIMERE we used that were triggered in our particular case, or the problem is purely hardware i.e. the writing of the file goes wrong because of memory access issues. The first possibility is not very likely since meteorological values between "ANH" and "APC" barely differ in terms of magnitude. Plus, these absurd values seem to appear randomly (in terms of variable / time step / geographic situation) for two identical runs. The second option is the most likely explanation so far since a run with a newer version of CHIMERE that cleaned some unused chemical cycles from the code failed only once and eventually went through. These unused cycles could explain that non allocated variables jumped into the results creating a mess in the output writing. The third possibility is currently under investigation since hardware issues have been detected by other members of the team.

Comparison with Other Studies

- A recent first implementation of WRF-CHIMERE-EDGAR over a Latin American country, namely Argentina, was studied in García Ferreyra et al., 2016. In this study, a country-wide 50km resolution simulation was run. They find a generally large underestimation of NO_x and $PM_{2.5}$ probably linked to the coarse resolution and the situation of the monitoring systems that may not be representative. They obtain a good reproduction of daily cycles though. According to the study, more data and a refined emissions inventory are needed for better results. These conclusions apply to our case as well.
- In Mazzeo et al., 2018 a similar approach to our study was implemented in order to assess the effects of cutting emissions from transport and/or residential sectors. The meteorological configuration used is close but the previous version of CHIMERE was used. They find a consistent difficulty to reproduce peak $PM_{2.5}$ events and also largely underestimate NO_x mixing ratios.
- Prospective studies on the impacts of IPCC RCP scenarios on air quality have been conducted for other regions of the world. Below are gathered some of their findings, which are consistent with the ones we find for Santiago.
  - United States (Zhang et al., 2017): in this study using the WRF/Chem coupled CTM, they include both changes in pollutants emissions and climate change implied by RCP4.5 and RCP8.5 scenarios. At the 2046-2055 horizon, they find for the continental US, that $PM_{2.5}$ concentrations are projected to decrease on average by $1.5\mu g/m^3$ (or 30%) in RCP4.5 scenario, due to decreased emissions of primary PM and precursors and increased precipitations. In RCP8.5 scenario they find an even stronger decrease with an average $1.7\mu g/m^3$ (or 35%) drop in $PM_{2.5}$ concentrations. They attribute this difference to larger decreases in Elemental Carbon and anthropogenic secondary organic aerosol on top of primary organic aerosol emissions increasing in RCP4.5 and decreasing in RCP8.5.
  - Europe (Colette et al., 2013): in this study they use CHIMERE under CMIP5 climate simulations, with RCP2.6 and RCP8.5 emission levels, over Western Europe. They find that the decrease of $PM_{2.5}$ by 2050 is very large under both scenarios, with average concentrations dropping by 8 and $9.8\mu g/m^3$ with respect to 2005 levels over Western Europe in the RCP8.5 and RCP2.6 scenarios, respectively. Locally, concentrations can even decrease by up to $20\mu g/m^3$. This decrease is mainly explained by a drop in secondary aerosols formation as a result of decreasing anthropogenic emission of precursors.
  - China (Li et al., 2016): this study uses GEOS-Chem model under the four IPCC RCP scenarios to simulate 2000-2050 changes in $PM_{2.5}$ concentrations in China, with a focus on the four main polluted regions of the country. Their findings include that under the RCP6.0 scenario, at the 2050 horizon, $PM_{2.5}$ concentrations will systematically increase, by as much as $+30\mu g/m^3$ in winter time. The three other scenarios show decreasing concentrations in 2050, the best scenario being the RCP4.5. RCP2.6 and RCP8.5 show comparable results around -10 to $-20\mu g/m^3$ in 2050 in winter time, although for the extremely polluted Sichuan Basin RCP2.6 is way better than RCP8.5.

Next steps

Below are summarized some points that leave room for improvement in the continuation of this project, and in particular during the associated PhD work.

- Work on improving the meteorological simulations outputs: we have seen in this study that simulated meteorology is very sensitive to the WRF configuration used in terms of physics, boundary layer schemes, resolution... It will be interesting to study other configurations to assess how much accuracy can be gained. We could use, for instance, the WRF configuration of the current forecast system in Santiago Schmitz and Falvey, 2006 or configurations used in other studies on Latin America. WRF v4.0 having just been released in June 2018 with updated schemes, a look at this new version could also be useful.
- In combination with better modeling, better on-site monitoring could be a real asset as well, as we have seen that some parts of the data showed weird numbers that we could not use.

- For future air quality projections purposes, it could be interesting to use a projected climate for the meteorological forcing. For instance, instead of using actual weather conditions as of 2016, a downscaling from LMDz climate projection as of 2050 could be used. CMIP5 results could also be an interesting source for future climate path as it provides ensemble mean projections. In addition, it could be interesting to run the same simulations with RCP emissions as of 2020 this time, and compare the results with measurements as of today in order to assess which scenario is closer to reality so far, i.e. whether we are taking RCP2.6 or RCP8.5 path in terms of air quality.
- This study focused mainly on winter time. Thus, a question would be to extend the simulations to a whole year in order to assess the performance of the model for other seasons, with a view to the implementation of a daily air quality forecast system in Santiago, based on CHIMERE.
- Significant work has yet to be done regarding emissions inventories of primary pollutants and precursors. We mentioned earlier that a major limitation for the reproduction of observed air quality is the lack of dynamical and updated emission schemes. For this, models such as Integrated Transportation and Land Use Models (ITLUM) could be interesting to look at. The stakes around better emission inventories have been well identified, in particular in the framework of the EMISA Project (International Global Atmospheric Chemistry, 2017).
- A personal question your writer asks himself relates to how much of the Black Carbon emitted in Santiago area reaches the close Andes mountains, and how this contributes to ice and snow melting (Molina et al., 2015, Hadley and Kirchstetter, 2012). In this respect, assessing the transport of BC from Santiago over the Andes using CHIMERE could be an interesting research topic.

Acknowledgement

First of all, I am really grateful to Sylvain Mailler, head of the InTro team at LMD, who made me discover the field of atmospheric chemistry during his extremely interesting lessons in the MEC655C course of the STEEM Graduate Degree. His teachings convinced me that these are the topics I want to deal with in my future career. What's more, he has been an outstanding supervisor, full of precious pieces of advice and commitment.

Laurent Menut also deserves a great deal of thankfulness for his support and all the knowledge he shared with me along the internship. I am absolutely convinced that Laurent and Sylvain will be outstanding PhD supervisors.

In his position of head of LMD and my academic supervisor, I am grateful to Philippe Drobinski for having me as an intern at LMD.

Finally, I would like to thank all the executives of the STEEM Graduate Degree for having me as a student this year. Thanks to this program I had the chance to find my way towards a career that is made for me.

Qi² Réseau de recherche Qualité de l'air en Ile-de-France

This internship has benefited from a funding by DIM Qi², emerging major field of interest in Ile-de-France region. Ce stage a bénéficié d'un financement du DIM Qi², Domaine d'intérêt majeur émergent de la région Ile-de-France.

References

[1] Airparif. Etude de la distribution spatiale des niveaux moyens d'ozone en periode estivale dans le secteur de rambouillet et dans la zone rurale sud-ouest de l'ile-de-france, 2001.

[2] Airparif. Etat initial de la qualité de l'air à Santiago du Chili avant la mise en place du projet Transantiago, 2006.

[3] Marcos Andrade-Flores, Nestor Rojas, Megan L. Melamed, Olga L. Mayol-Bracero, Michel Grutter, Laura Dawidowski, Juan Carlos Antuña-Marrero, Carlos Rudamas, Laura Gallardo, Ruben Mamani-Paco, Maria de Fatima Andrade, and Nicolàs Huneeus. Fostering a collaborative atmospheric chemistry research community in the Latin America and Caribbean region. *American Meteorological Society*, 2016.

[4] Banco Central de Chile. Base de Datos Estadísticos, 2018. URL `https://si3.bcentral.cl/Siete/secure/cuadros/home.aspx`.

[5] F. Barraza, F. Lambert, H. Jorquera, A.M. Villalobos, and L. Gallardo. Temporal evolution of main ambient PM2.5 sources in Santiago, Chile, from 1998 to 2012. *Atmos. Chem. Phys.*, 2017. doi: 10.5194/acp-17-10093-2017.

[6] Berkeley Earth. Berkeley earth, 2018. URL `http://berkeleyearth.org/`.

[7] M. Bocquet, H. Elbern, H. Eskes, M. Hirtl, R. Zabkar, G. R. Carmichael, J. Flemming, A. Inness, M. Pagowski, J. L. Pérez Camaño, P. E. Saide, R. San Jose, M. Sofiev, J. Vira, A. Baklanov, C. Carnevale, G. Grell, and C. Seigneur. Data assimilation in atmospheric chemistry models: current status and future prospects for coupled chemistry meteorology models. *Atmos. Chem. Phys.*, 2015. doi: 10.5194/acp-15-5325-2015.

[8] Yuyu Chen, Avraham Ebenstein, Michael Greenstone, and Hongbin Li. Evidence on the impact of sustained exposure to air pollution on life expectancy from China's Huai River policy. *Proceedings of the National Academy of Science of the United States of America*, 2013.

[9] Aaron J. Cohen, Michael Brauer, Richard Burnett, H Ross Anderson, Joseph Frostad, Kara Estep, Kalpana Balakrishnan, Bert Brunekreef, Lalit Dandona, Rakhi Dandona, Valery Feigin, Greg Freedman, Bryan Hubbell, Amelia Jobling, Haidong Kan, Luke Knibbs, Yang Liu, Randall Martin, Lidia Morawska, C Arden Pope III, Hwashin Shin, Kurt Straif, Gavin Shaddick, Matthew Thomas, Rita van Dingenen, Aaron van Donkelaar, Theo Vos, Christopher J L Murray, and Mohammad H Forouzanfar. Estimates and 25-year trends of the global burden of disease attributable to ambient air pollution: an analysis of data from the Global Burden of Diseases Study 2015. *Lancet*, 2017. doi: 10.1016/S0140-6736(17)30505-6.

[10] A. Colette, B. Bessagnet, R. Vautard, S. Szopa, S. Rao, S. Schucht, Z. Klimont, L. Menut, G. Clain, F. Meleux, G. Curci, and L Rouil. European atmosphere in 2050, a regional air quality and climate perspective under CMIP5 scenarios. *Atmos. Chem. Phys.*, 2013. doi: 10.5194/acp-13-7451-2013.

[11] Christopher G. Collier. *Hydrometeorology*. John Wiley and Sons, 2016.

[12] William D. Collins, Philip J. Rasch, Byron A. Boville, James J. Hack, James R. McCaa, David L. Williamson, Jeffrey T. Kiehl, Bruce Briegleb, Cecilia Bitz, Shian-Jiann Lin, Minghua Zhang, and Yongjiu Dai. Description of the NCAR Community Atmosphere Model (CAM 3.0). Technical report, National Center for Atmospheric Research, 2004.

[13] Paola Crippa, Ryan C. Sullivan, Abhinav Thota, and Sara C. Pryor. The impact of resolution on meteorological, chemical and aerosol properties in regional simulations with WRF-Chem. *Atmos. Chem. Phys.*, 2017. doi: 10.5194/acp-17-1511-2017.

[14] Jimy Dudhia. Numerical Study of Convection Observed during th Winter Monsoon Experiment Using a Mesoscale Two-Dimensional Model. *Journal of the Atmospheric Sciences*, 1989.

[15] Encyclopædia Britannica. Atmospheric circulation meteorology, 2018. URL `https://www.britannica.com/science/atmospheric-circulation`.

[16] Energy Policy Institute at the University of Chicago. Air Quality Life Index, 2017. URL `https://aqli.epic.uchicago.edu/`.

[17] EU Copernicus. Macc project - documentation on regional systems, 2018. URL `http://www.gmes-atmosphere.eu/about/documentation/regional/`.

[18] European Commission. Prediction of Air Pollution in Latin America, 2018. URL `https://cordis.europa.eu/project/rcn/212962_fr.html`.

[19] European Environment Agency. Emissions of primary particles and secondary particulate matter precursors, 2009. URL `https://www.eea.europa.eu/data-and-maps/indicators/emissions-of-primary-particles-and-1/emissions-of-primary-particles-and-1`.

[20] Mark Falvey and René D. Garreaud. Regional cooling in a warming world: Recent temperature trends in the southeast Pacific and along the west coast of subtropical South America (1979-2006). *Journal of Geophysical Research*, 2009. doi: 10.1029/2008JD010519.

[21] Laura Gallardo, Francisco Barraza, Andrés Ceballos, Mauricio Galleguillos, Nicolás Huneeus, Fabrice Lambert, Cecilia Ibarra, Marcela Munizaga, Raúl O'Ryan, Mauricio Osses, Sebastián Tolvett, Anahí Urquiza, and Karina D. Véliz. Evolution of air quality in Santiago: The role of mobility and lessons from the science-policy interface. *Elem. Sci. Anth.*, 2018. doi: 10.1525/elementa.293.

[22] M.F. García Ferreyra, G. Curci, and M. Lanfri. First Implementation of the WRF-CHIMERE-EDGAR Modeling System Over Argentina. *IEEE Journal of Selected Topics in Applied Earth Observations and Remote Sensing*, 2016. doi: 10.1109/JSTARS.2016.2588502.

[23] Paul Ginoux, Joseph M. Prospero, Thomas E. Gill, N. Christina Hsu, and Ming Zhao. Global-scale attribution of anthropogenic and natural dust sources and their emission rates based on MODIS DEEP BLUE aerosol products. *Reviews of Geophysics*, 50, RG3005, 2012.

[24] G. A. Grell and S. R. Freitas. A scale and aerosol aware stochastic convective parameterization for weather and air quality modeling. *Atmos. Chem. Phys. Discuss.*, 2013. doi: 10.5194/acpd-13-23845-2013.

[25] Georg A. Grell and Dezso Dévényi. A generalized approach to parameterizing convection combining ensemble and data assimilation techniques. *Geophysical Research Letters*, 2002. doi: 10.1029/2002GL015311.

[26] Odelle L. Hadley and Thomas W. Kirchstetter. Black-carbon reduction of snow albedo. *Nature Climate Change*, 2012. doi: 10.1038/NCLIMATE1433.

[27] Song-You Hong and Jeong-Ock Jade Lim. The WRF Single-Moment 6-Class Microphysics Scheme (WSM6). *Journal of the Korean Meteorological Society*, 2006.

[28] Song-You Hong, Jimy Dudhia, and Shu-Hua Chen. A Revised Approach to Ice Microphysical Processes for the Bulk Parameterization of Clouds and Precipitation. *American Meteorological Society*, 2004.

[29] Song-You Hong, Yign Noh, and Jimy Dudhia. A New Vertical Diffusion Package with an Explicit Treatment of Entrainment Processes. *American Meteorological Society*, 2006.

[30] International Cryosphere Climate Initiative. Andes and black carbon, 2018. URL `http://iccinet.org/andes-and-black-carbon`.

[31] International Global Atmospheric Chemistry. Emissions in south america, 2017. URL `http://www.igacproject.org/activities/emisa`.

[32] IPCC. RCP Database, 2009. URL `http://www.iiasa.ac.at/web-apps/tnt/RcpDb`.

[33] Laboratoire de Météorologie Dynamique. CHIMERE web page, 2018. URL `http://www.lmd.polytechnique.fr/chimere/`.

[34] Ke Li, Hong Liao, Jia Zhu, and Jonathan M. Moch. Implications of RCP emissions on future PM 2.5 air quality and direct radiative forcing over China. *Journal of Geophysical Research: Atmospheres*, 121, 2016. doi: 10.1002/2016JD025623.

[35] S. Mailler, L. Menut, D. Khvorostyanov, M. Valari, F. Couvidat, G. Siour, S. Turquety, R. Briant, P. Tuccella, B. Bessagnet, A. Colette, L. Létinois, K. Markakis, and F. Meleux. Chimere-2017: from urban to hemispheric chemistry-transport modeling. *Geoscientific Model Development*, 10(6): 2397–2423, 2017. doi: 10.5194/gmd-10-2397-2017.

[36] S. Makowski Giannoni, K. Trachte, R. Rollenbeck, L. Lehnert, J. Fuchs, and J. Bendix. Atmospheric salt deposition in a tropical mountain rainforest at the eastern Andean slopes of south Ecuador - Pacific or Atlantic origin? *Atmos. Chem. Phys.*, 16:10241–10261, 2016. doi: 10.5194/acp-16-10241-2016.

[37] Andrea Mazzeo, Nicolàs Huneeus, César Ordoñez, Andrea Orfanoz-Cheuquelaf, Laurent Menut, Sylvain Mailler, Myrto Valari, Hugo Denier van der Gon, Laura Gallardo, Ricardo Muñoz, Rodrigo Donoso, Maurico Galleguillos, Mauricio Ossesa, and Sebastian Tolvett. Impact of residential combustion and transport emissions on air pollution in Santiago during winter. *Atmospheric Environment*, 2018. doi: 10.1016/j.atmosenv.2018.06.043.

[38] Ministerio del Medio Ambiente. Análisis General para el Impacto Económico y Social (AGIES) de la Norma de Calidad Primaria de Material Particulado 2.5. *Ambiente MdM*, 2012.

[39] Ministerio del Medio Ambiente. Establece norma primaria de calidad ambiental para material particulado fino respirable mp2.5, 2012. URL `https://www.leychile.cl/Navegar?idNorma=1025202&idVersion=2012-01-01`.

[40] Ministerio del Medio Ambiente. Planes de Descontaminación Atmosférica, 2018. URL `http://portal.mma.gob.cl/tag/planes-de-descontaminacion-atmosferica/`.

[41] Ministerio del Medio Ambiente. Sistema de Información Nacional de Calidad del Aire, 2018. URL `https://sinca.mma.gob.cl/index.php/`.

[42] Eli J. Mlawer, Steven J. Taubman, Patrick D. Brown, Michael J. Iacono, and Shepard A. Clough. Radiative transfer for inhomogeneous atmospheres: RRTM, a validated correlated-k model for the longwave. *Journal of Geophysical Research*, 1997. doi: 0148-0227/97/97JD-00237509.00.

[43] L.T. Molina, L. Gallardo, M. Andrade, Baumgardner, M. Borbor-Córdova, R. Bórquez, G. Casassa, F. Cereceda-Balic, L. Dawidowski, R. Garreaud, N. Huneeus, F. Lambert, J.L. McCarty, J. Mc Phee, M. Mena-Carrasco, G.B. Raga, C. Schmitt, and J.P. Schwarz. Pollution and its impacts on the South American Cryosphere (PISAC). *Earth's Future*, 2015. doi: eft2.2015EF000311.

[44] Aldo Montecinos and Patricio Aceituno. Seasonality of the ENSO-Related Rainfall Variability in Central Chile and Associated Circulation Anomalies. *Journal of Climate*, 2003.

[45] Mikio Nakanishi and Hiroshi Niino. An Improved Mellor-Yamada Level-3 Model: its Numerical Stability and Application to a Regional Prediction of Advection Fog. *Boundary-Layer Meteorology*, 2006. doi: 10.1007/s10546-005-9030-8.

[46] National Center for Atmospheric Research. Weather Research and Forecasting Model, 2018. URL `https://www.mmm.ucar.edu/weather-research-and-forecasting-model`.

[47] NOAA. National Oceanic and Atmospheric Administration - US DoC, 2018. URL `http://www.noaa.gov/`.

[48] OECD. The Economic Consequences of Outdoor Air Pollution. *OECD Publishing*, 2016. doi: 10.1787/9789264257474-en.

[49] Axel Osses, Laura Gallardo, and Tania Faundez. Analysis and evolution of air quality monitoring networks using combined statistical information indexes. *Tellus B: Chemical and Physical Meteorology*, 2013. doi: 10.3402/tellusb.v65i0.19822.

[50] C. A. Paulson. The Mathematical Representation of Wind Speed and Temperature Profiles in the Unstable Atmospheric Surface Layer. *Journal of Applied Meteorology*, 1970.

[51] H. Petetin, M. Beekmann, A. Colomb, H. A. C. Denier van der Gon, J.-C. Dupont, C. HonorÃ©, V. Michoud, Y. Morille, O. Perrussel, A. Schwarzenboeck, J. Sciare, A. Wiedensohler, and Q. J. Zhang. Evaluating BC and NOx emission inventories for the Paris region from MEGAPOLI aircraft measurements. *Atmos. Chem. Phys.*, 2015. doi: 10.5194/acp-15-9799-2015.

[52] C. Rafenberg, G. Dixsaut, and I. Annesi-Maesano. Evaluation a minima du coût de la pollution atmosphérique pour le système de soin français. *Environ Risque Santé*, 2015. doi: 10.1684/ers.2015.0769.

[53] Keywan Riahi, Shilpa Rao, Volker Krey, Cheolhung Cho, Vadim Chirkov, Guenther Fischer, Georg Kindermann, Nebojsa Nakicenovic, and Peter Rafaj. RCP 8.5-A scenario of comparatively high greenhouse gas emissions. *Climatic Change*, 2011. doi: 10.1007/s10584-011-0152-.

[54] Juan J. Ruiz, Celeste Saulo, and Julia Nogués-Paegle. WRF Model Sensitivity to Choice of Parameterization over South America: Validation against Surface Variables. *American Meteorological Society*, 2010. doi: 10.1175/2010MWR3358.1.

[55] Pablo E. Saide, Marcelo Mena-Carrasco, Sebastian Tolvett, Pablo Hernandez, and Gregory R. Carmichael. Air quality forecasting for winter-time $PM_{2.5}$ episodes occurring in multiple cities in central and southern Chile. *Journal of Geophysical Research: Atmospheres*, 2016. doi: 10.1002/2015JD023949.

[56] P.E. Saide, S.N. Spak, G.R. Carmichael, M.A. Mena-Carrasco, Q. Yang, S. Howell, D.C. Leon, J.R. Snider, A.R. Bandy, J.L. Collett, K.B. Benedict, S.P. de Szoeke, L.N. Hawkins, G. Allen, I. Crawford, J. Crosier, and S.R. Springston. Evaluating WRF-Chem aerosol indirect effects in Southeast Pacific marine stratocumulus during VOCALS-REx. *Atmos. Chem. Phys.*, 2012. doi: 10.5194/acp-12-3045-2012.

[57] Rainer Schmitz and Mark Falvey. Numerical Air Quality Forecasting in Santiago de Chile. *Proceedings of 8 ICSHMO*, 2006.

[58] William C. Skamarock, Joseph B. Klemp, Jimy Dudhia, David O. Gill, Dale M. Barker, Michael G. Duda, Xiang-Yu Huang, Wei Wang, and Jordan G. Powers. A Description of the Advanced Research WRF Version 3. *NCAR Technical Note*, 2008.

[59] Efisio Solazzo, Roberto Bianconi, Christian Hogrefe, Gabriele Curci, Paolo Tuccella, Ummugulsum Alyuz, Alessandra Balzarini, Rocío Baró, Roberto Bellasio, Johannes Bieser, Jorgen Brandt, Jesper H. Christensen, Augustin Colette, Xavier Francis, Andrea Fraser, Marta Garcia Vivanco, Pedro Jiménez-Guerrero, Ulas Im, Astrid Manders, Uarporn Nopmongcol, Nutthida Kitwiroon, Guido Pirovano, Luca Pozzoli, Marje Prank, Ranjeet S. Sokhi, Alper Unal, Greg Yarwood, and Stefano Galmarini. Evaluation and error apportionment of an ensemble of atmospheric chemistry transport modeling systems: multivariable temporal and spatial breakdown. *Atmos. Chem. Phys.*, 2017. doi: 10.5194/acp-17-3001-2017.

[60] Task Force on Hemispheric Transport of Air Pollution. HTAP website, 2014. URL `http://edgar.jrc.ec.europa.eu/htap_v2/index.php`.

[61] M. Tewari, F. Chen, W. Wan, J. Dudhia, M. A. LeMone, K. Mitchell, M. Ek, G. Gayno, J. Wegiel, and R. H. Cuenca. Implementation and Verification of the Unified NOAH Land Surface Model in the WRF Model. *20th conference on weather analysis and forecasting/16th conference on numerical weather prediction*, 2004.

[62] The USGS Land Cover Institute. The usgs land cover institute, 2016. URL `https://landcover.usgs.gov/`.

[63] The World Bank Group. Climate change knowledge portal 2.0, 2018. URL `http://sdwebx.worldbank.org/climateportal/`.

[64] United Nations. World Population Prospects 2017, 2017. URL `https://esa.un.org/unpd/wpp/`.

[65] United Nations Development Programme. Human Development Report 2016, 2016.

[66] Detlef P. van Vuuren, Elke Stehfest, Michel G. J. den Elzen, Tom Kram, Jasper van Vliet, Sebastiaan Deetman, Morna Isaac, Kees Klein Goldewijk, Andries Hof, Angelica Mendoza Beltran, Rineke Oostenrijk, and Bas van Ruijven. RCP2.6: exploring the possibility to keep global mean temperature increase below 2°C. *Climatic Change*, 2011. doi: 10.1007/s10584-011-0152-3.

[67] Ana M. Villalobos, Francisco Barraza, Héctor Jorquera, and James J. Schauer. Chemical speciation and source apportionment of fine particulate matter in Santiago, Chile, 2013. *Science of the Total Environment*, 2015. doi: 10.1016/j.scitotenv.2015.01.006.

[68] Hong Wang, Xiaoye Zhang, Yao Peng, Hongli Liu, Meng Zhang, and Huizheng Che. The Contributions to the Explosive Growth of PM 2.5 Mass due to Aerosols-Radiation Feedback and Further Decrease in Turbulent Diffusion during a Red-alert Heavy Haze in JING-JIN-JI in China. *Atmos. Chem. Phys. Discuss.*, 2018. doi: 10.5194/acp-2018-512.

[69] World Health Organization. Disability-adjusted life year (daly), 2018. URL `http://www.who.int/healthinfo/global_burden_disease/metrics_daly/en/`.

[70] World Health Organization. 9 out of 10 people worldwide breathe polluted air, but more countries are taking action, 2018. URL `http://www.who.int/news-room/detail/02-05-2018`.

[71] World Meteorological Organization. World weather information service, 2017. URL `http://worldweather.wmo.int/en/city.html?cityId=103`.

[72] Hongbin Yu, Mian Chin, Tianle Yuan, Huisheng Bian, Lorraine A. Remer, Joseph M. Prospero, Ali Omar, David Winker, Yuekui Yang, Yan Zhang, Zhibo Zhang, and Chun Zhao. The fertilizing role of African dust in the Amazon rainforest: A first multiyear assessment based on data from Cloud-Aerosol Lidar and Infrared Pathfinder Satellite Observations. *American Geophysical Union*, 2015. doi: 10.1002/2015GL063040.

[73] Yang Zhang, Kai Wang, and Chinmay Jena. Impact of Projected Emission and Climate Changes on Air Quality in the U.S.: from National to State Level. *Procedia Computer Science*, 110, 2017. doi: 10.1016/j.procs.2017.06.074.

[74] Yuqiang Zhang, Jared H. Bowden, Zachariah Adelman, Vaishali Naik, Larry W. Horowitz, Steven J. Smith, and J. Jason West. Co-benefits of global and regional greenhouse gas mitigation for US air quality in 2050. *Atmospheric Chemistry and Physics*, 16, 2016. doi: 10.5194/acp-16-9533-2016.